



**PRECISE CALCULATION OF COMPLEX
RADIOACTIVE DECAY CHAINS**

THESIS

Logan J. Harr, Captain, USAF

AFIT/GNE/ENP/07-03

**DEPARTMENT OF THE AIR FORCE
AIR UNIVERSITY**

AIR FORCE INSTITUTE OF TECHNOLOGY

Wright-Patterson Air Force Base, Ohio

APPROVED FOR PUBLIC RELEASE; DISTRIBUTION UNLIMITED

The views expressed in this thesis are those of the author and do not reflect the official policy or position of the United States Air Force, Department of Defense, or the United States Government.

AFIT/GNE/ENP/07-03

PRECISE CALCULATION OF COMPLEX RADIOACTIVE DECAY CHAINS

THESIS

Presented to the Faculty

Department of Engineering Physics

Graduate School of Engineering and Management

Air Force Institute of Technology

Air University

Air Education and Training Command

In Partial Fulfillment of the Requirements for the
Degree of Master of Science (Nuclear Engineering)

Logan J. Harr, B.S.

Captain, USAF

March 2007

APPROVED FOR PUBLIC RELEASE; DISTRIBUTION UNLIMITED.

PRECISE CALCULATION OF COMPLEX RADIOACTIVE DECAY CHAINS

Logan J. Harr, B.S.
Captain, USAF

Approved:



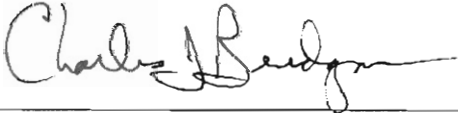
Kirk A. Mathews (Chairman)

15 Mar 2007
date



David W. Gerts (Member)

7 Mar 2007
date



Charles J. Bridgman (Member)

14 March 2007
date

Abstract

This thesis documents a new approach to investigate the gamma radiation activity of the fission products of three different fuels (U-235, U-238, and U-239) exposed to three different incident neutron energy spectra (thermal, fast spectrum, and high energies). An application of the exponential moments function is used with a transmutation matrix in the calculation of complex radioactive decay chains to achieve greater precision than can be attained through current methods. The result of this research is a code which can calculate the decay products from complex radioactive decay chains with a high degree of precision while quantifying the uncertainty in gamma activity due to uncertainties in the isotope properties.

Acknowledgments

Work on this thesis has been nearly a year long effort. I want to thank my wife for her patience and understanding throughout the entirety of this process. I also wish to recognize my advisor, Dr. Mathews, for the amount of time and effort he gave me in working out the inevitable bugs in my code. Special thanks also go to Dr. Gerts for his help in increasing my understanding of the Fortran language.

Logan J. Harr

Table of Contents

	Page
Abstract.....	iv
<i>Acknowledgments</i>	v
<i>List of Figures</i>	viii
<i>List of Tables</i>	x
<i>I. Introduction</i>	1
I.A: Motivation.....	2
I.B: Statement of the Problem.....	3
I.C: Goal of the Research.....	3
I.D: Scope.....	3
I.E: Assumptions	4
<i>II. Analysis and Approach</i>	5
II.A: Special Radioactive Decay Problem.....	5
II.B: Solution Methods of the Special Problem	7
1. Bateman Solution Formula	8
2. Numerical Integration of Coupled ODEs	9
3. Matrix Exponential (Transmutation Matrix) Method.....	10
4. Transmutation Matrix by Exponential Moments Function	11
II.C: Generalization to the Full Problem.....	15
<i>III. Implementation</i>	18
III.A: Input Data	18
1. Isotope Decay Information	18
2. Gamma Radiation Data.....	20
3. $N(0)$ Data	21
III.B: Decay Chain Identification	22
III.C: Exponential Moments Function Implementation	23
1. One Argument	24
2. Two Arguments	24
3. Three Arguments	25
4. N Arguments.....	26
III.D: T-matrix Generation	27

	Page
III.E: Calculating $N(t)$	28
III.F: Calculating $A(E,t)$	29
<i>IV. Verification Process</i>	31
IV.A: Defining the Range of Calculation Inputs	31
IV.B: Creating the Calculation Inputs	33
IV.C: Verifying the Calculations.....	33
IV.D: Verifying the Depth First Search Routine	35
<i>V. Monte Carlo Estimation of Uncertainty</i>	37
<i>VI. Performance, Results, and Analysis</i>	39
VI.A: Performance	39
VI.B: $A(E,t)$	41
1. Total Activity	43
2. 1-2 MeV	54
3. 2-3 MeV	58
4. 3-4 MeV	64
5. 4-5 MeV	68
6. 5-6 MeV	73
7. 6-7 MeV	79
8. 7-8 MeV	83
9. >8 MeV	86
<i>VII. Conclusions and Recommendations</i>	87
VII.A: Conclusions.....	87
VII.B: Recommendations for Future Work	88
Appendix A: Order Invariance of Bateman Equation	89
Appendix B: Depth-First Search Verification Test Problems	90
Appendix C: Mathematica Verification Notebook.....	91
Bibliography	92

List of Figures

Figure	Page
1. Functional Code Schematic	5
2. Complex Radioactive Decay Chain	15
3. Depth First Search Chain Identification	23
4. Matrix Storage of Eight Fission Product Yield Vectors at t=0.....	28
5. Histogram of Database Gamma Energies (200 keV bins)	30
6. Histogram for Gamma Energies >5 MeV (200 keV bins).....	30
7. Time to Generate T-matrix for Given Time Steps.....	40
8. Energy Bin Contributions to Activity for U-235 Thermal.....	42
9. Total Activity, 1 nanosecond to 10 seconds, Log-Linear	44
10. Total Activity, 1 nanosecond to 10 seconds, Semi-Log	47
11. Total Activity, 1 nanosecond to 25,000 years, Semi-Log.....	50
12. Total Activity, 10 s to 25000 years, Log-Log.....	51
13. Dose Rate and the Way-Wigner Approximation	53
14. Activity, 1-2 MeV Gammas, 1 ns to 10 s, Log-Linear	55
15. Activity, 1-2 MeV Gammas, 1 ns to 10 s, Semi-Log	56
16. Activity, 1-2 MeV, 1 ns to 25,000 y, Semi-Log	57
17. Gamma Activity, 2-3 MeV, 1 ns to 10 s, Log-Linear.....	59
18. Gamma Activity, 2-3 MeV, 10 s to 25000 y, Log-Log	60
19. Gamma Activity with Uncertainty, 2-3 MeV, 1 day to 3 weeks	62
20. Gamma Activity, 3-4 MeV, 1 ns to 10 s, Log-Linear.....	65
21. Gamma Activity, 3-4 MeV, 1 ns to 100 y, Log-Log	66

Figure	Page
22. Gamma Activity, 3-4 MeV, 1 ns to 100 y, Semi-Log.....	67
23. Gamma Activity, 4-5 MeV, 1 ns to 10 s, Log-Linear.....	69
24. Gamma Activity, 4-5 MeV, 1 ns to 10 s, Semi-Log.....	70
25. Gamma Activity, 4-5 MeV, 10 s to 10 ⁶ s, Log-Log	71
26. Gamma Activity, 4-5 MeV, 1 s to 1.2*10 ⁶ s, Semi-Log.....	72
27. Gamma Activity, 5-6 MeV, 1 ns to 10 s, Log-Linear.....	74
28. Gamma Activity, 5-6 MeV, 1 ns to 10 s, Semi-Log.....	75
29. Gamma Activity, 5-6 MeV, 10 s to 10 ⁶ s, Log-Log	78
30. Gamma Activity, 6-7 MeV, 1 ns to 10 s, Log-Linear.....	80
31. Gamma Activity, 6-7 MeV, 10 s to 10,000 s, Log-Log.....	81
32. Gamma Activity, 6-7 MeV, 10 s to 6,000 s, Semi-Log	82
33. Gamma Activity, 7-8 MeV, 1 ns to 10 s, Log-Linear.....	84
34. Gamma Activity, 7-8 MeV, 1 s to 1,200 s, Semi-Log	85

List of Tables

Table	Page
1. Sample NuDat2 Output for Hydrogen, Deuterium, and Tritium	19
2. Fission Product Isotopes with Large Relative Uncertainties	20
3. Sample Input Gamma Data.....	21
4. Major Contributors to Total Activity at 4.64×10^{-5} s and Half Lives	48
5. Fission Product Yield per Fission Type.....	76
6. Rb-92 Quantity per Fission at t=0 s and t=3 s	76

PRECISE CALCULATION OF COMPLEX RADIOACTIVE DECAY CHAINS

I. Introduction

The activity of radioactive isotopes is based on two factors: the quantity of the isotope present and the half life of the isotope. This thesis attempts to document a methodology for improving the calculated activity through increased precision of the calculation of each isotope at any given time and direct calculation of the radioactivity. Also, the propagation of uncertainty in the activity due to the uncertainties in the isotope data is quantified through a Monte Carlo method.

The half lives of isotopes span many orders of magnitude, from short-lived isotopes that decay nearly instantaneously to stable isotopes with very long half lives. Because of the large range of half lives, calculating the quantity of each isotope present in a given decay chain after a period of time may be difficult due to the stiffness the differential equations describing radioactive decay. To avoid this stiffness, solutions are most commonly found by making approximations. In this typical implementation, isotopes are evaluated differently based on the magnitude of the half life in relation to other isotopes in the chain and the position of the isotope in the chain (the first isotope in the chain versus an isotope near the end of the chain).

For some applications, models find gamma activity by using an approximation that the gamma activity decays as $t^{-1.2}$. This approximation is used for any arbitrary

gamma energy range as well as total activity. The new model seeks to improve upon this approximation by calculating the activity directly for each time step for any given energy bin.

This chapter outlines the motivation for developing a new method for use in radioactive decay calculations, the goal of the research, the scope of the problem I attempted to solve, and the assumptions made in developing this new implementation of the exponential moments function.

I.A: Motivation

A more robust method of calculating radioactive decays is desired to increase the precision of the results. A method which treats all isotopes the same, regardless of position in the chain or relative magnitude, will treat decay chains uniformly and therefore more predictably and with greater precision.

It is important to know the quantities of each isotope remaining after a given time more precisely than available with current methods. This will allow for more precise calculation of the activity of the radioactive isotopes and lead to a better understanding of high energy gammas emitted following the neutron induced fission of uranium and plutonium isotopes.

The Way-Wigner approximation is that the dose rate, \dot{D} , following thermal fission of U-235 falls off as

$$\dot{D}(t) = \dot{D}(1)t^{-1.2} \quad (1.1)$$

where $\dot{D}(t)$ is the dose rate at any unit time[4:2]. We examine the accuracy of this approximation as applied to various fuels, spectra of neutrons that induce fission, and gamma radiation energy groups.

I.B: Statement of the Problem

Precisely model the time-dependent gamma spectrum produced by the neutron induced fission of three different isotopes with three different energy neutrons while quantifying the gamma activity uncertainty due to uncertainties of the isotope half lives. Develop computer programs that are useful tools for performing such studies.

I.C: Goal of the Research

The goal of this research is to more precisely characterize the gamma activity following a fission event by using the exponential moments function in a radioactive decay code to calculate the quantity of isotopes remaining at some given time with precision. This research also attempts to quantify the propagation of uncertainty in the gamma activity caused by uncertainties in both the half lives of isotopes and gamma decay intensities.

I.D: Scope

The scope of this research is limited to creating a decay code for all isotopes with fewer than 99 protons (californium and below). Isotopes with higher Z numbers can be used, but the amount of information available for elements above californium drops off significantly.

Fissionable nuclei considered here are limited to uranium-235, uranium-238, and plutonium-239. For each of these isotopes three different incident neutron spectra are evaluated: thermal neutrons, fast fission spectrum neutrons, and high-energy neutrons. Because U-238 does not fission by absorbing a thermal neutron, a total of eight different test cases are evaluated.

The specified time step for the code can be any number between 1.0 nanosecond and 25,000 years.

I.E: Assumptions

The fission product lists were taken from text files created by T.R. England and B.F. Rider and made available on the Lawrence Berkely Laboratory website [5]. These files contain the atomic number and symbol of the isotope, as well as an indication if the isotope is in its ground state or a metastable state. For each metastable state listed, I assumed that this corresponded to the most excited metastable state found in the NuDat 2.0 data files. If an isotope listed as a fission product does not appear in the NuDat 2.0 data, I assumed that it instantly underwent successive beta decays until reaching an isotope for which there is data.

II. Analysis and Approach

A functional schematic of the approach used to solve the complex decay chain problem is shown in Figure 1. The white boxes represent the formatted text files containing user input data and code output files. The shaded boxes show the macroscopic processes performed by the code.

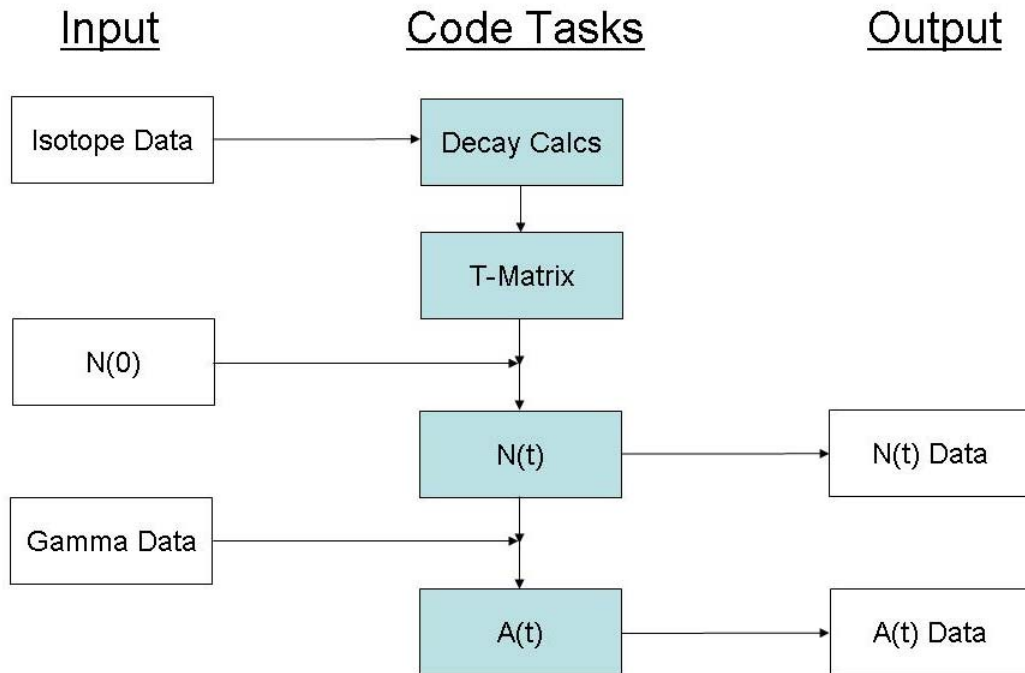


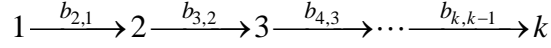
Figure 1 Functional Code Schematic

The rest of this chapter is dedicated to a discussion of radioactive decay theory and examining the macroscopic code tasks in greater detail.

II.A: Special Radioactive Decay Problem

The special radioactive decay problem describes the decay of an initial quantity of a single radioactive isotope that is not being replenished and decays through a single

chain (without branching). Schematically, this can be represented using generic isotopes 1, 2, 3, and so on to an arbitrary depth ending in the k^{th} isotope.



The branching fractions (i.e. $b_{2,1}$) are all equal to unity for the special decay problem.

The decay of the initial isotope 1 is described by the differential equation

$$\dot{N}_1(t) + \lambda_1 N_1(t) = 0 \quad (2.1)$$

where λ_1 and $N_1(t)$ are the decay constant and quantity of isotope 1 at time t . The differential equation for the quantity of isotope 2 is similarly given by

$$\dot{N}_2(t) + \lambda_2 N_2(t) = b_{2,1} \lambda_1 N_1(t). \quad (2.2)$$

This method can be generalized for the decay chain of arbitrary length k as

$$\dot{N}_k(t) + \lambda_k N_k(t) = b_{k,k-1} \lambda_{k-1} N_{k-1}(t) \quad (2.3)$$

The special radioactive decay problem for the sample isotope decay can be represented as a lower-triangular matrix as in equation (2.4):

$$\begin{pmatrix} \dot{N}_1(t) \\ \dot{N}_2(t) \\ \dot{N}_3(t) \\ \vdots \\ \dot{N}_{k-1}(t) \\ \dot{N}_k(t) \end{pmatrix} + \begin{pmatrix} \lambda_1 & 0 & 0 & \dots & 0 & 0 \\ -b_{2,1}\lambda_1 & \lambda_2 & 0 & \dots & 0 & 0 \\ 0 & -b_{2,1}\lambda_1 & \lambda_3 & \dots & 0 & 0 \\ \vdots & \vdots & \vdots & \ddots & \vdots & \vdots \\ 0 & 0 & 0 & 0 & \lambda_{k-1} & 0 \\ 0 & 0 & 0 & 0 & -b_{k,k-1}\lambda_{k-1} & \lambda_k \end{pmatrix} \begin{pmatrix} N_1(t) \\ N_2(t) \\ N_3(t) \\ \vdots \\ N_{k-1}(t) \\ N_k(t) \end{pmatrix} = \dot{\vec{N}}(t) + \Lambda \vec{N}(t) = 0. \quad (2.4)$$

One solution to equation (2.4) is of the form

$$\vec{N}(t) = e^{-\Lambda t} \vec{N}(0). \quad (2.5)$$

By defining the transmutation matrix, or T-matrix, as

$$\mathbb{T}(t) \equiv e^{-\Lambda t}, \quad (2.6)$$

the solution to equation (2.4) can alternatively be expressed as

$$\vec{N}(t) = \mathcal{T}(t)\vec{N}(0). \quad (2.7)$$

The advantage of this formulation is that elements of the T-matrix are calculated individually and the solution is calculated using matrix operations. This takes advantage of the low memory requirements for individual element calculations with the speed of optimized matrix multiplications. The solution method used to calculate the values of each element of the T-matrix affects the efficiency, accuracy, and precision of the results.

The calculation of the activity is straightforward once $\vec{N}(t)$ is known. The activity for the special decay problem produced by any isotope is defined as the product of the decay constant and the quantity. A subset of the total activity of interest in this thesis is the gamma activity. Using the concept of the transmutation matrix introduced above, the gamma activity can be calculated by

$$\vec{A}(t) = \mathcal{G}\mathcal{T}(t)\vec{N}(0) = \mathcal{G}\vec{N}(t). \quad (2.8)$$

Individual elements of the gamma matrix are populated by calculating the product of the decay constant and the intensity of the radiation. The radiation intensity indicates the probability of a specific gamma ray being emitted for a given decay process. Because the radiation intensity is given for each gamma radiation, it possible to sort the gamma activity by energy bins specified in the code by the user.

II.B: Solution Methods of the Special Problem

I investigated four different approaches to solving the radioactive decay differential equations: the Bateman solution formula, numerical integration of the

ordinary differential equation, matrix exponentiation, and Mathew's solution in exponential moments functions [7].

1. Bateman Solution Formula

The most common way of solving the differential equations that describe radioactive decay is known as the Bateman solution. The Bateman solution is easily derived using Laplace transforms as shown in numerous nuclear engineering texts (1:76-78). The Bateman solution formulates the solution to equation (2.1) as

$$N_1(t) = N_1(0)e^{-\lambda_1 t} . \quad (2.9)$$

The solution to the second differential equation begins by recognizing that the right hand side of equation (2.2) includes $N_1(t)$ which is known explicitly from equation (2.9).

Making this substitution and algebraically manipulating the result leads to the solution for the quantity of the second isotope

$$N_2(t) = b_{2,1}\lambda_1 N_1(0) \left(\frac{e^{-\lambda_1 t}}{(\lambda_2 - \lambda_1)} + \frac{e^{-\lambda_2 t}}{(\lambda_1 - \lambda_2)} \right) . \quad (2.10)$$

Generically applying this formula to the last (k^{th}) isotope in a decay chain yields the Bateman solution formula:

$$N_k(t) = N_1(0) \left(\prod_{i=1}^{k-1} b_{i+1,i} \lambda_i \right) \sum_{j=1}^k \frac{e^{-\lambda_j t}}{\prod_{\substack{i=1 \\ i \neq j}}^k (\lambda_i - \lambda_j)} . \quad (1.11)$$

The principle advantage of the Bateman solution is the straightforwardness of the approach. The formulation makes it easy to implement into a computer code with nested DO loops to handle the summation and product operations.

The denominator of the Bateman solution however involves a subtraction between the decay constants of the isotopes in the decay chain. When the decay constants are very close together, catastrophic cancellation occurs resulting in a shrinking denominator which causes the loss of digits of precision. Implemented into a computer code directly, this loss of precision leads to significant errors in the final result.

2. Numerical Integration of Coupled ODEs

Another approach to obtaining the answer to the decay problem is to use a numerical integration method to solve the coupled, linear, first order differential equations directly. For small, well defined problems, the primary advantage of this solution is that the loss of precision inherent in the Bateman equation when $\lambda_i \approx \lambda_j$ is avoided by solving the differential equations directly.

The advantage of this approach is offset by the large computational resources which are necessary to simultaneously solve individual decay chains and the stiffness which results when λ_i and λ_j differ by many orders of magnitude. Scaling this beyond the scope of limited test problems to calculate all of the decays of interest to this thesis would be prohibitive given the 3,443 unique isotopes and more than 68,000 unique decay chains. The NDSolve built-in routine in Mathematica [9] was used to numerically solve the differential decay equations for a series of test problems representative of the actual decay isotope data using up to 200 digits of working precision and with decay chains up to four isotopes deep. Even under this limited test condition the numerical integration solution displayed numerical instability and took hundreds of times longer to calculate than other methods.

3. Matrix Exponential (Transmutation Matrix) Method

The matrix exponential method is used to solve a system of linear first order differential equations with constant coefficients. This method represents the system of equations below

$$\begin{aligned}
 N_1'(t) &= -\lambda_1 N_1(t), & N_1(0) &= N_1^0 \\
 N_2'(t) &= b_{2,1}\lambda_1 N_1(t) - \lambda_2 N_2(t), & N_2(0) &= 0 \\
 &\vdots & &\vdots \\
 N_k'(t) &= b_{k-1,k}\lambda_2 N_2(t) - \lambda_k N_k(t), & N_k(0) &= 0
 \end{aligned} \tag{2.12}$$

in the matrix form

$$\vec{N}'(t) = \mathcal{C}\vec{N}(t), \quad \vec{N}(0) = \vec{N}^0 \tag{2.13}$$

where \mathcal{C} is the square coefficient matrix of order k. The solution to equation (2.13) is of the form

$$\vec{N}(t) = e^{t\mathcal{C}}\vec{N}(0) \tag{2.14}$$

and can be solved through use of a matrix of the change basis as described in *Matrix Theory and Linear Algebra* [6:376-405]. ORIGEN uses this type of formulation to make its calculations in the method shown in equation (2.15), where $t\mathcal{C} = \mathbb{A}$.

$$\begin{aligned}
 e^{\mathbb{A}}N &= \left(I + \mathbb{A} + \frac{\mathbb{A}^2}{2!} + \frac{\mathbb{A}^3}{3!} + \dots \right) N \\
 &= N + \mathbb{A}N + \frac{\mathbb{A}}{2}(\mathbb{A}N) + \frac{\mathbb{A}}{3}\left(\frac{\mathbb{A}}{2}(\mathbb{A}N)\right) + \dots
 \end{aligned} \tag{2.15}$$

The advantage of using the second equation is that the computer never has to multiply anything larger than a matrix on a vector, reducing the computational cost of this method.

The series can be expanded to as many terms as needed to achieve the desired precision.

The formulation of the problem as a transmutation matrix is a useful construct. In practice, however, performing matrix operations on a square matrix of order equal to the total number of isotopes is computationally too expensive to perform on a desktop computer without making the approximations used in ORIGEN.

4. Transmutation Matrix by Exponential Moments Function

The solution method presented in this section was provided by Mathews [7]. It uses that exponential moments functions that were developed by Mathews and his students [8]. They were designed in the context of developing discrete ordinates transport methods but can be applied to the problem of radioactive decay to avoid the catastrophic loss of precision of the Bateman solution. The moments function in its most general case is defined as

$$M_n(\lambda_1, \lambda_2, \dots, \lambda_k) = \int_0^1 dt_1 \int_0^{t_1} dt_2 \dots \int_0^{t_{k-1}} dt_k (1-t_1)^n e^{-\lambda_1 t_1} e^{(\lambda_1 - \lambda_2) t_2} \dots e^{(\lambda_{k-1} - \lambda_k) t_k}. \quad (2.16)$$

For the radioactive decay problem, the unforced $n = 0$ or M_0 solution is used.

$$M_0(\lambda_1, \lambda_2, \dots, \lambda_k) = \int_0^1 dt_1 \int_0^{t_1} dt_2 \dots \int_0^{t_{k-1}} dt_k e^{-\lambda_1 t_1} e^{(\lambda_1 - \lambda_2) t_2} \dots e^{(\lambda_{k-1} - \lambda_k) t_k}. \quad (2.17)$$

The exponential moments function solution is suited to this application because it can take advantage of a recurrence relation to calculate the solution for a chain of any length.

After multiplying both sides of equation (2.2) by $e^{\lambda_2 t_1}$, the quantity of isotope 2 at any given time can be determined as above by integrating over the time of interest.

$$\left[\dot{N}_2(t_1) + \lambda_2 N_2(t_1) \right] e^{\lambda_2 t_1} = b_{2,1} \lambda_1 N_1(t_1) e^{\lambda_2 t_1} = \frac{d}{dt_1} \left(N_2(t_1) e^{\lambda_2 t_1} \right) \quad (1.18)$$

$$\int_0^{t_2} \frac{d}{dt_1} \left(N_2(t_1) e^{\lambda_2 t_1} \right) dt_1 = N_2(t_2) e^{\lambda_2 t_2} - N_2(0) = \int_0^{t_2} \frac{d}{dt_1} b_{2,1} \lambda_1 N_1(t_1) e^{\lambda_2 t_1} dt_1 \quad (1.19)$$

$$N_2(t_2) = b_{2,1} \lambda_1 e^{-\lambda_2 t_2} \int_0^{t_2} dt_1 N_1(t_1) e^{\lambda_2 t_1} \quad (1.20)$$

But, $N_1(t_1)$ is known from equation (2.9). Substituting this back into equation (1.20)

yields

$$N_2(t_2) = b_{2,1} \lambda_1 e^{-\lambda_2 t_2} \int_0^{t_2} dt_1 N_1(0) e^{-\lambda_1 t_1} e^{\lambda_2 t_1} = b_{2,1} \lambda_1 e^{-\lambda_2 t_2} \int_0^{t_2} dt_1 N_1(0) e^{-(\lambda_1 - \lambda_2) t_1} \quad (1.21)$$

The equation for any isotope j along the chain follows the same form as equation (1.21).

$$N_j(t_j) = b_{j,j-1} \lambda_{j-1} e^{-\lambda_j t_j} \int_0^{t_j} dt_{j-1} N_{j-1}(t_{j-1}) e^{\lambda_j t_{j-1}} \quad (2.22)$$

Substituting solutions for $N_{j-1}(t_{j-1})$ into equation (2.22) and rearranging terms reveals a nested structure to the solution

$$N_j(t_j) = b_{j,j-1} b_{j-1,j-2} \lambda_{j-1} \lambda_{j-2} e^{-\lambda_j t_j} \int_0^{t_j} dt_{j-1} \left(e^{-(\lambda_{j-1} - \lambda_j) t_{j-1}} \int_0^{t_{j-1}} dt_{j-2} N_{j-2}(t_{j-2}) e^{\lambda_j t_{j-2}} \right) \quad (2.23)$$

that can be extended to the generic case of k isotopes

$$N_k(t) = \left(\prod_{i=1}^{k-1} b_{i+1,i} \lambda_i \right) e^{-\lambda_k t} \int_0^t dt_{k-1} e^{-(\lambda_{k-1} - \lambda_k) t_{k-1}} \int_0^{t_{k-1}} dt_{k-2} e^{-(\lambda_{k-2} - \lambda_{k-1}) t_{k-2}} \dots \int_0^{t_2} dt_1 N_A(0) e^{-(\lambda_1 - \lambda_2) t_1} \quad (2.24)$$

Multiplying and dividing through by t and performing a change of variables where

$$u_j = t_j / t \text{ and } \int_0^{t_j} \frac{dt_{j-1}}{t} = \int_0^{u_j} du_{j-1} \text{ then rearranging terms produces equation (2.25)}$$

$$N_k(t) = N_1(0) \left(\prod_{i=1}^{k-1} b_{i+1,i} \lambda_i t \right) e^{-\lambda_k t} \int_0^1 du_{k-1} e^{-(\lambda_{k-1} t - \lambda_k t) u_{k-1}} \int_0^{u_{k-1}} du_{k-2} e^{((\lambda_{k-1} t - \lambda_k t) - (\lambda_{k-2} t - \lambda_k t)) u_{k-2}} \dots$$

$$\dots \int_0^{u_2} du_1 e^{((\lambda_2 t - \lambda_k t) - (\lambda_1 t - \lambda_k t)) u_1} \quad (2.25)$$

Now applying the exponential moments function to equation (2.25) in the solution of the differential equations describing radioactive decay, the quantity of the k^{th} isotope can be represented by

$$N_k(t) = N_1(0) \left(\prod_{i=1}^{k-1} b_{i+1,i} \lambda_i t \right) e^{-\lambda_k t} M_0 [(\lambda_{k-1} t - \lambda_k t), (\lambda_{k-2} t - \lambda_k t), \dots, (\lambda_1 t - \lambda_k t)]. \quad (2.26)$$

After some algebraic manipulations of equations (1.11) and (2.26), the Bateman and exponential moments function solutions can be expressed as a ratio of the quantity of isotope k to the initial quantity of isotope 1.

$$\frac{N_k(t)}{N_1(0)} = \left(\prod_{i=1}^{k-1} b_{i+1,i} \lambda_i t \right) \sum_{j=1}^k \frac{e^{-\lambda_j t}}{\prod_{\substack{i=1 \\ i \neq j}}^k (\lambda_i t - \lambda_j t)} \quad (2.27)$$

$$= \left(\prod_{i=1}^{k-1} b_{i+1,i} \lambda_i t \right) e^{-\lambda_k t} M_0 [(\lambda_{k-1} t - \lambda_k t), (\lambda_{k-2} t - \lambda_k t), \dots, (\lambda_1 t - \lambda_k t)]$$

Equation (2.27) shows that the exponential moments function and the modified Bateman equation have a common product in parentheses. Dividing through by the common

product, I define a new function, $F(\vec{\lambda}t)$, dependent upon the vector of decay constants and time:

$$\begin{aligned}
 F(\vec{\lambda}t) &\equiv \sum_{j=1}^k \frac{e^{-\lambda_j t}}{\prod_{\substack{i=1 \\ i \neq j}}^k (\lambda_i t - \lambda_j t)} \\
 &\equiv e^{-\lambda_k t} M_0 \left[(\lambda_{k-1} t - \lambda_k t), (\lambda_{k-2} t - \lambda_k t), \dots, (\lambda_1 t - \lambda_k t) \right]
 \end{aligned} \tag{2.28}$$

Algebraic manipulation of the Bateman solution (Appendix A) shows that it, and hence $F(\vec{\lambda}t)$, is invariant with respect to argument order. This is important because it means that the decay constants can be sorted by size before performing the calculation. By sorting the decay constants from largest to smallest, the moments-function form of $F(\vec{\lambda}t)$ can be rewritten as

$$F(\vec{\lambda}t) = e^{-\lambda_{smallest} t} M_0 \left[\vec{\lambda}_{\substack{\text{excluding} \\ \text{smallest}}} t - \lambda_{smallest} t \right]. \tag{2.29}$$

This ensures that every argument passed to the exponential moments function is greater than or equal to zero. If the arguments passed to the moments-function are all non-negative, then $0 \leq M_0 \leq 1$, eliminating overflow errors.

The final form of the equation used to determine the quantity of isotopes in the decay chain at time t is therefore

$$\frac{N_k(t)}{N_1(0)} = \left(\prod_{i=1}^{k-1} b_{i,i+1} \lambda_i t \right) e^{-\lambda_{smallest} t} M_0 \left[\vec{\lambda}_{\substack{\text{excluding} \\ \text{smallest}}} t - \lambda_{smallest} t \right]. \tag{2.30}$$

II. C: Generalization to the Full Problem

To this point, the branching fractions have been assumed to be unity for the special radioactive decay problem. In reality, many radioactive isotopes have multiple decay mechanisms resulting in branching ratios between 0 and 1. Figure 2 gives an example of a more complex decay scheme. Here isotopes 1 and 2 have multiple decay mechanisms, isotope 5 is produced from more than one parent isotope, and isotopes 4 and 6 are stable.

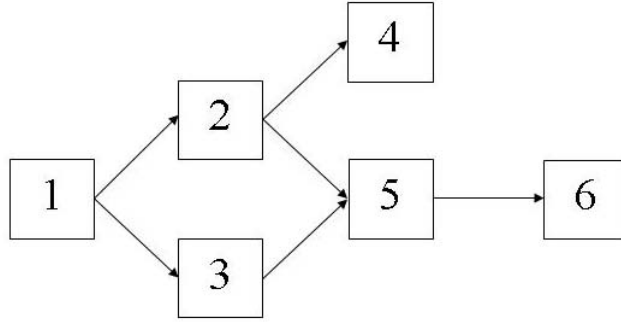


Figure 2 Complex Radioactive Decay Chain

The system of differential equations describing this more complex decay scheme is shown in equation (2.31).

$$\begin{pmatrix} \dot{N}_1(t) \\ \dot{N}_2(t) \\ \dot{N}_3(t) \\ \dot{N}_4(t) \\ \dot{N}_5(t) \\ \dot{N}_6(t) \end{pmatrix} + \begin{pmatrix} \lambda_1 & 0 & 0 & 0 & 0 & 0 \\ -b_{2,1}\lambda_1 & \lambda_2 & 0 & 0 & 0 & 0 \\ -b_{3,1}\lambda_1 & 0 & \lambda_3 & 0 & 0 & 0 \\ 0 & -b_{4,2}\lambda_2 & 0 & 1 & 0 & 0 \\ 0 & -b_{5,2}\lambda_2 & -b_{5,3}\lambda_3 & 0 & \lambda_5 & 0 \\ 0 & 0 & 0 & 0 & -b_{6,5}\lambda_5 & 1 \end{pmatrix} \begin{pmatrix} N_1(t) \\ N_2(t) \\ N_3(t) \\ N_4(t) \\ N_5(t) \\ N_6(t) \end{pmatrix} = \dot{\vec{N}}(t) + \Lambda \vec{N}(t) = 0 \quad (2.31)$$

It follows from this that the transmutation matrix must then be equal to

$$T(t) \equiv e^{-\Lambda t} = \begin{bmatrix} \frac{N_1(t)}{N_1(0)} & 0 & 0 & 0 & 0 & 0 \\ \frac{N_2(t)}{N_1(0)} & \frac{N_2(t)}{N_2(0)} & 0 & 0 & 0 & 0 \\ \frac{N_3(t)}{N_1(0)} & 0 & \frac{N_3(t)}{N_3(0)} & 0 & 0 & 0 \\ \frac{N_4(t)}{N_1(0)} & \frac{N_4(t)}{N_2(0)} & 0 & 1 & 0 & 0 \\ \frac{N_5(t)}{N_1(0)} & \frac{N_5(t)}{N_2(0)} & \frac{N_5(t)}{N_3(0)} & 0 & \frac{N_5(t)}{N_5(0)} & 0 \\ \frac{N_6(t)}{N_1(0)} & \frac{N_6(t)}{N_2(0)} & \frac{N_6(t)}{N_3(0)} & 0 & \frac{N_6(t)}{N_5(0)} & 1 \end{bmatrix} \quad (2.32)$$

where the individual elements are calculated using equation (2.30).

The generalization of the problem using 6 isotopes in the example above is directly scalable to the full scope of the thesis with 3,443 isotopes. The T-matrix for the full problem is sparse (composed of a vast majority of elements with a value of 0) and is not a lower triangular matrix.

Once the T-matrix is created, the quantity of each isotope at time t is determined using equation (2.7) and taking advantage of the MATMUL built-in function in the Fortran compiler. Following the determination of $\vec{N}(t)$, the calculation of the gamma activity at time t is straightforward using the gamma activity matrix introduced for the special decay problem above. However, elements of \mathcal{G} are now calculated as:

$$g_{ij} = \lambda_j \sum_k \left(b_{k,j} \sum_l I_{l,k}(E_i) \right). \quad (2.33)$$

g_{ij} is the gamma activity due to radioactive decay in energy bin i from isotope j. λ_j is the decay constant for isotope j. $b_{k,j}$ is the branching ratio for the decay from isotope j to

any isotope k that results in a gamma ray emission. $I_{l,k}(E_i)$ is the intensity of the radiation line l in energy bin i resulting from the decay of isotope j into isotope k .

III. Implementation

The gamma ray activity code is made up of five main sub tasks: the depth-first search used to identify all of the daughter isotopes in a chain, the decay algorithm implementing the exponential moments function, the generation of the T-matrix, the calculation of the quantities of each isotope, and finally the calculation of the gamma ray activity rate. The rest of this chapter discusses the data necessary to run the code and then examines the functioning of each one of the 5 sub tasks in detail.

III.A: Input Data

The data required to run the code are: radioactive decay data including the decay mode and half life with uncertainties for every isotope, gamma decay data including gamma energies, decay modes, and intensities with uncertainties, and a list of initial quantities of isotopes, $\overline{N}(0)$. The decay code is designed to work with any set of input data as long as it is in the proper format. The individual processes were verified using test problem sets containing completely generic data, as will be discussed in more detail in Chapter IV. This means that performance of the code is solely dependent upon the quality of the data that is used to characterize the problem.

1. Isotope Decay Information

Isotopic decay data was taken from NuDat 2.0, an interactive web based program developed by the National Nuclear Data Center (NNDC). NuDat 2.0 produces a text output of all isotope decays with data obtained from the Evaluated Nuclear Structure

Data File (ENSDF). The NNDC maintains the ENSDF file and currently lists 3,165 different isotopes and more than 80,000 gamma rays. The difference in the number of isotopes maintained by the NNDC and the number of isotopes used in the decay code (3,443) is due to the accounting of metastable isotope states. The NNDC counts all metastable states as one isotope, whereas the decay code assigns a different isotope number to each metastable state for tracking purposes.

An example of the NuDat 2.0 output is below in Table 1. The only changes made to the table from the original data are that columns containing information on the spin and uncertainties in the mass excess energy and natural abundance have been omitted for readability. The uncertainties are contained in the text version of the half life and given in the Nuclear Data Sheets style [5]. In the case of tritium, the half life is 12.32 ± 0.02 years.

Table 1 Sample NuDat2 Output for Hydrogen, Deuterium, and Tritium

A	Element	Z	N	Mass Exc (MeV)	T ½ (txt)	T ½ (s)	Abundance (%)	Decay Mode	Branching Ratio (%)
1	H	1	0	7.289	STABLE	Infinity	99.99		
2	H	1	1	13.136	STABLE	Infinity	0.01		
3	H	1	2	14.95	12.32 Y 2	3.89E+08	0	B-	100

Several problems were encountered in using the NuDat 2.0 output data for a decay code. The purpose of the database is to provide as much information to a user as possible, while for the purposes of writing a decay code, the quantity of data is not the most important factor. What instead is needed is the information that produces complete decay chains. For example, Ni-48 undergoes electron capture to Co-48; however no isotope information is available on Co-48. The best way I found for dealing with this problem was to create a dummy isotope with zero protons and zero neutrons. All decays

for which no daughter isotope information exist default decay into this imaginary isotope. This ensures that the correct amount of the parent isotope decays away with each time step. However, this treatment of unknown daughter isotopes effectively allows leaking from the system in that the mass of recognized isotopes at $t = 0$ may not be equal to the mass of the recognized isotopes at $t = t_1$. To track this problem an error log is created for each program run that lists the isotopes with missing decay daughter information.

Another problem with the data is the half life uncertainties. The uncertainties are given as a σ , or standard deviation, for a Gaussian distribution [10]. However, the uncertainties listed for isotopes can not be a σ because half lives can not be less than zero. When the relative uncertainty is small compared to the half life, this approximation may be adequate because many multiples of the uncertainty must be subtracted from the listed half live to create a negative half life and this possibility is exceedingly unlikely. However, 66 different isotopes have half lives and uncertainties within 3σ of 0. Table 2 lists the three fission product isotopes within three standard deviations of 0. This problem is handled using rejection sampling and is discussed in greater detail in Chapter V.

Table 2 Fission Product Isotopes with Large Relative Uncertainties

A	Symbol	Half Life (s)	Uncertainty (s)
66	Cr	0.010	0.006
70	Co	0.50	0.18
76	Ni	0.24	0.24

2. Gamma Radiation Data

Gamma radiation information is also available through NuDat 2.0. The first four data fields are the same as in the isotope data file. Additional fields include information

on the decay, radiation type, radiation energy, intensity, and dose, each listed with the appropriate uncertainties. A sample of the gamma input data follows.

Table 3 Sample Input Gamma Data

A	Sym	Z	N	Decay Mode	T ½ (txt)	T ½ (s)	Rad Type	Rad E (keV)	σ	Rad Intensity (%)	σ
8	He	2	6	B-	119.1 MS 12	0.119	G	980		84	10
7	Be	4	3	EC	53.22 D 6	5E+06	G	477.6	20	10.44	4
8	B	5	3	B+	770 MS 3	0.77	G	511		12	12

The gamma data specifies what type of decay produces the gamma radiation (internal transition, β^- , β^+ , etc.). The code treats initial quantities of metastable states correctly in that internal transition decays and the associated gamma emission are counted. Subsequent decay mechanisms in the code do not populate metastable states because all decays are assumed to produce a nucleus in the ground state. This approach was selected because of the lack of data completely describing the decay process through metastable states. While this introduces errors into the code results, most metastable state half lives are very short compared to the half lives of the ground state nuclei, so the error is not intolerable.

3. $N(0)$ Data

Fission product yield data for uranium-235, uranium-238, and plutonium 239 were taken from work by T.R. England and B.F. Rider [5]. They define the thermal neutron spectra as neutron energies which are in thermal equilibrium with the surroundings present in a light water reactor. Fast neutron fission products are the yields caused by fission spectrum neutrons. High energy neutrons come from the

${}^3_1\text{H} + {}^2_1\text{H} \rightarrow {}^4_2\text{He} + n$ (D-T) reaction and have energy of 14.07 MeV [3:29].

I chose to use fission product yields as population sets for the initial values of $\bar{N}(0)$ because of the large number of different isotopes produced in these reactions. The fission of U-235 by thermal neutrons produces 776 different isotopes. This provides complex data sets with well documented results.

III.B: Decay Chain Identification

The depth-first search is initiated by sending the decay chain algorithm a starting isotope. If the isotope is stable then the algorithm exits. However, in the case of a radioactive isotope, the algorithm identifies the number of mechanisms by which the isotope decays. Each one of the decay mechanisms results in a separate recursive call to the decay chain algorithm, tracking the new generation information as well as adding the decay constant and the branching ratio for that decay to global storage vectors. The algorithm recursively calls itself until a stable isotope is reached at the end of the chain.

Upon completing the chain by finding a stable isotope, the vectors containing the branching ratios and decay constants are passed to the decay calculation routine. Once the decay calculations are performed, the algorithm backs up one level and either completes the process for the next branching mechanism or passes a new branching ratio and decay constant vectors to the decay calculation algorithm (now each reduced in size by one).

The performance of the depth first search is illustrated by returning to the sample decay scheme introduced in Figure 2. Figure 3 lists each decay chain for the sample complex decay scheme in the order in which they are identified. The figure also shows

the branching fraction vector and decay constant vector passed to the decay calculation subroutine.

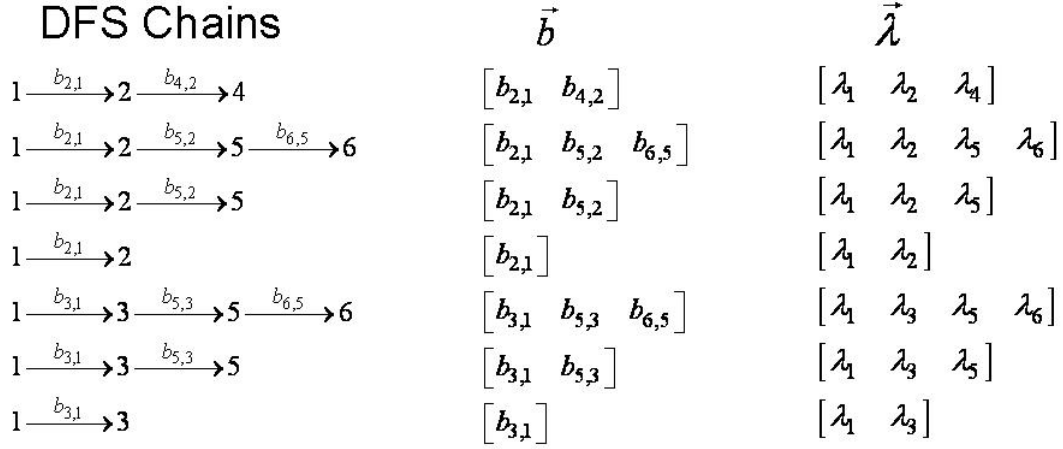


Figure 3 Depth First Search Chain Identification

III. C: Exponential Moments Function Implementation

Before making a call to the exponential moments function routine, the $\vec{\lambda}t$ vector which consists of all positive and decreasing values, must be created by multiplying each decay constant in the chain by the time of interest. For the sake of clarity, I now define a new vector \vec{x} where

$$\vec{x} = \vec{\lambda}_{\text{excluding smallest}} t - \lambda_{\text{smallest}} t. \quad (3.1)$$

The \vec{x} vector is created by sorting $\vec{\lambda}t$ by size, and subtracting the smallest value from every other value in the vector. Once this is accomplished, the exponential moments function routine is called and the solution method is based on the number of arguments in \vec{x} .

1. One Argument

The simplest call to the exponential moments function solution is for a vector of length one and is given by

$$M_0(\vec{x}) = M_0(x_1) = \frac{1 - e^{-x_1}}{x_1}. \quad (3.2)$$

Implementing this into the code is straightforward, but even here care is taken to minimize any loss of precision. Clearly, if x_1 is large the numerator approaches 1.0. Computational time can be saved by avoiding the expensive exponential calculation when the numerator will equal 1.0 to the specified precision. For double precision (16 digits of precision), this occurs for values of $x_1 > 36.8414$. The code uses the approximation in equation(3.3) for all instances where $x_1 > 38.0$.

$$M_0(x_1) \cong \frac{1}{x_1} \quad (3.3)$$

At the other extreme is values of x_1 which are small. Small values can cause a loss of precision in the numerator as the exponential term approaches 1.0 which is amplified by then dividing by the small number. To avoid this a series expansion is performed up for values of $x_1 < 0.1$. For instances where x_1 is neither small nor large, the default exponential moments function formulation, equation (3.2), is used.

2. Two Arguments

For a vector of size two, the moments function can be expressed as a relationship between the exponential moments function of the individual arguments. The two arguments are sorted such that $x_1 \leq x_2$.

$$M_0(\vec{x}) = M_0(x_1, x_2) = \frac{M_0(x_2) - M_0(x_1)}{x_1 - x_2} \quad (3.4)$$

The same logic used in the single argument case above can be extended here, and if

$x_2 > 38.0$ (since \vec{x} is sorted, this also means that $x_1 > 38.0$) then

$$M_0(x_1, x_2) = \frac{1}{x_1 x_2}. \quad (3.5)$$

Likewise, if both arguments are small, the Taylor series expansion is used to cancel terms and avoid loss of precision.

There is also a new case that must be investigated. If x_1 and x_2 are neither both small nor both large, then a case may arise where they are close together, and if not dealt with correctly, leaves the same problem which is so destructive to the precision of the Bateman equation. Here though the exponential moments function formulation can be re-expressed using a change of variable $x_2 = x_1 + dx$ to eliminate the subtraction in the denominator.

$$M_0(x_1, x_1 + dx) = \frac{M_0(x_1 + dx) - M_0(x_1)}{x_1 - (x_1 + dx)} = \frac{M_0(x_1) - e^{-x_1} M_0(dx)}{x_2} \quad (3.6)$$

3. Three Arguments

If all three of the arguments are large, the inverse product approximation is used. If all three of the arguments are small, a series expansion is used. For the case of three arguments where either two of the arguments or all of the arguments are close together, the following equation is used to evaluate the arguments once the arguments are sorted into increasing order ($x_1 \leq x_2 \leq x_3$).

$$M_0(x_1, x_2, x_3) = \frac{M_0(x_1, x_2) - e^{-x_1} M_0(x_2 - x_1, x_3 - x_1)}{x_3} \quad (3.7)$$

In the general case, the 3rd kind exponential moments function is handled by equation (3.8).

$$M_0(x_1, x_2, x_3) = \frac{(1 - \chi)M_0(x_1) - M_0(x_2) + \chi M_0(x_3)}{\chi(1 - \chi)(x_3 - x_1)^2}, \chi = \frac{x_2 - x_1}{x_3 - x_1} \quad (3.8)$$

4. N Arguments

For all times of interest in the implementation of this code, there are never more than three not all large, not all small, close together arguments. Therefore, given a chain of n decays the decay calculation can be expressed as a recursive use of the exponential moments function, dividing \vec{x} into subvectors of the original arguments. Assuming that the arguments are sort such that $x_1 \geq x_2 \geq \dots \geq x_n$,

$$M_0(\vec{x}) = M_0(x_1, x_2, \dots, x_n) = \frac{M_0(x_1, \dots, x_{n-1}) - M_0(x_2, \dots, x_n)}{x_n - x_1}. \quad (3.9)$$

Similarly to the specific argument cases of the exponential moments function introduced above, when the arguments are either all large or all small, an inverse product or a series expansion is used. If neither of these conditions are met, the moments function is then called recursively until the arguments passed into the moments function are all large, all of the arguments are small, or vectors of length one, two, or three are the only size vectors remaining.

III.D: T-matrix Generation

The purpose behind the T-matrix is to be able to perform a matrix multiplication on a vector of the initial quantities of isotopes to produce the remaining quantities of all isotopes. The T-matrix is initialized as an identity matrix with order k (where k = the total number of isotopes). For a stable isotope number j where $1 \leq j \leq k$, the T-matrix value will remain 1.0 at position (j,j) in the matrix and no calculations are performed on any element in the isotope column.

Each radioactive parent isotope is passed to the depth first search routine. Once a chain is completely identified, the information is passed to a decay calculation routine which calls the exponential moments function. The value along the diagonal is calculated directly for every radioactive isotope using

$$\frac{N_j(t)}{N_j(0)} = e^{-\lambda_j t} . \quad (3.10)$$

Values in the T-matrix in general will always be between 0.0 and 1.0. The only exceptions to this are decay processes that result in more than one of the same type of particle. For example, lithium-3 undergoes a decay which results in the emission of two protons, effectively undergoing a spontaneous fission with three hydrogen atoms produced by each decay of a lithium-3 atom. In this case, the T-matrix value (hydrogen-1, lithium-3) would approach 3.0 for any time of interest much greater than the half life of lithium-3 ($7.56 \cdot 10^{-23}$ s).

Decay mechanisms that result in the emission of neutrons, protons, or alpha particles have these particles tracked as well. For example, decay by proton emission to a

daughter isotope is also recorded as decaying to hydrogen. This ensures that the baryon count is conserved throughout the decay code.

III.E: Calculating $N(t)$

Once the T-matrix has been created for a time step t , finding the quantity of each isotope at time t is straightforward. First introduced in equation (2.7), calculating $N(t)$ is computed directly through matrix multiplication of the T-matrix and the initial quantities vector, $N(0)$.

$$\vec{N}(t) = \mathcal{T}(t)\vec{N}(0) \quad (3.11)$$

An advantage of using the T-matrix is that several problems can be investigated simultaneously as long as each problem is specified by its own $\vec{N}(0)$ vector. The number of vectors of initial quantities of atoms is represented by columns of data in an initial quantity matrix. To demonstrate this ability, all eight problem sets I wished to investigate were contained in separate columns of the $N(0)$ matrix as in Figure 4.

$$\begin{aligned} N(:,1) &= \vec{N}(0) : \text{U-235,thermal neutrons} \\ N(:,2) &= \vec{N}(0) : \text{U-235,fast neutrons} \\ N(:,3) &= \vec{N}(0) : \text{U-235,high energy neutrons} \\ N(:,4) &= \vec{N}(0) : \text{U-238,fast neutrons} \\ N(:,5) &= \vec{N}(0) : \text{U-238,high energy neutrons} \\ N(:,6) &= \vec{N}(0) : \text{Pu-239,thermal neutrons} \\ N(:,7) &= \vec{N}(0) : \text{Pu-239,fast neutrons} \\ N(:,8) &= \vec{N}(0) : \text{Pu-239,high energy neutrons} \end{aligned}$$

Figure 4 Matrix Storage of Eight Fission Product Yield Vectors at $t=0$

The series of $\vec{N}(0)$ vectors can be combined into an $N(0)$ matrix, changing equation (3.11) to

$$N(t) = T(t)N(0). \quad (3.12)$$

The Fortran built-in function MATMUL, when called with the arguments of the T-matrix and $N(0)$ matrix, performs this calculation more efficiently than possible through direct coding of the function.

III.F: Calculating $A(E,t)$

Gamma radiation information was taken from the NuDat 2 database by looking for all decays that produced gammas. The 80,125 results produced by this search are used to populate the data for calculation of the gamma activity produced by the range of isotopes of interest to this thesis. Gamma energies in the database range from 76.5 eV to 11.2589 MeV, with the bulk of these occurring at the lower energies. For example, there are only three gammas of over 10.0 MeV in the database, and all of them are produced through the β^+ decay of sodium-20. The distribution of gammas, broken down into 200 keV bins is shown in Figure 5 and Figure 6 below.

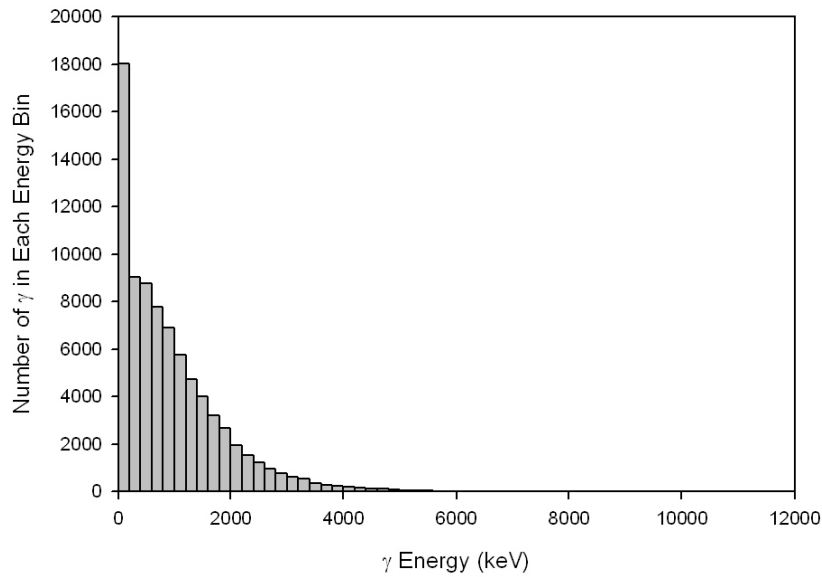


Figure 5 Histogram of Database Gamma Energies (200 keV bins)

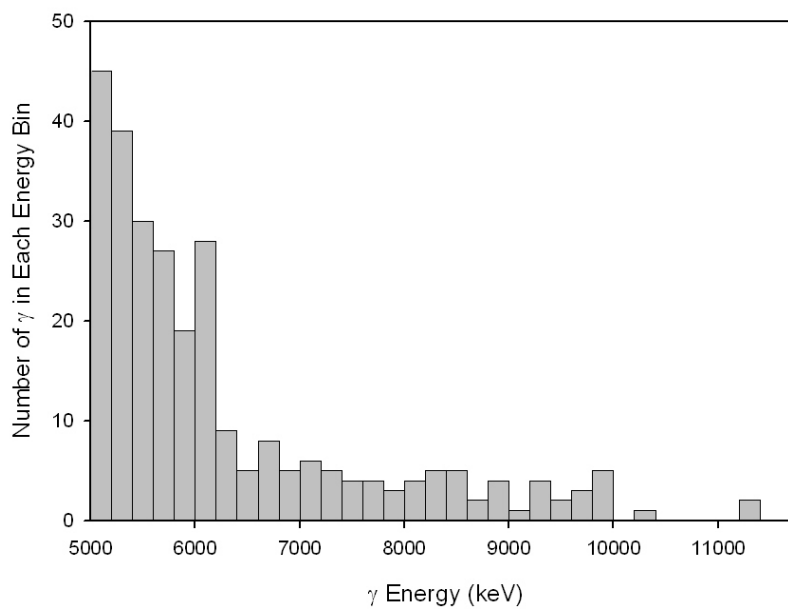


Figure 6 Histogram for Gamma Energies >5 MeV (200 keV bins)

Any number of energy bins can be specified and defined by the user in the input file, 'ProblemData.txt'. The energy bins are defined by a minimum and maximum bin energy given in keV. Applying the energy bin construct to the matrix formulation of the decay problem results in $\mathbb{A}(E, t) = \mathcal{G}(E)T(t)\mathbb{N}(0) = \mathcal{G}(E)\mathbb{N}(t)$.

IV. Verification Process

This research attempts to increase the precision of current exponential decay schemes by implementing the exponential moments function. This means that a thorough verification process had to be designed and implemented to ensure that the new code was producing the high precision results anticipated. Verification was accomplished using a comprehensive set of test problems that covered the entire range of potential anticipated inputs to the exponential moments function as well as various decay chains and gamma radiation decay energies and intensities. Mathematica was used as a benchmark for the solutions by performing calculations with greater than machine precision.

IV.A: Defining the Range of Calculation Inputs

The range of the test problems used for verification was bounded by the extremes of the decay constants found in the nuclear data tables and by the anticipated range of time steps. Isotopes of interest range from hydrogen ($Z=1$) to californium ($Z=98$). The shortest half-life in the problem scope is Li-3 with a half life of 7.56×10^{-23} s. At the other end of the spectrum are the stable nuclides, each with effective half lives of infinity. In practical terms, the exponential moments function will be validated using the longest lived radioactive isotope, Ge-76, with a half life of 3.79×10^{32} s. Therefore, the decay constant, λ , is bounded between $1.83 \times 10^{-33} \text{ s}^{-1}$ and $9.17 \times 10^{21} \text{ s}^{-1}$. Tests were also performed using $\lambda = 0$ for the stable isotopes, but values between the 0 and $1.83 \times 10^{-33} \text{ s}^{-1}$ were not explored.

Verification testing is also limited to time steps ranging between a nanosecond and 25000 years (7.94×10^{11} s). Time steps greater than this were not tested but are not expected to produce inaccurate results. This is because the longer time step sends increasingly more arguments to the large argument approximation of the exponential moments function and this approximation becomes better as the arguments become larger.

Because the exponential moments function deals with the differences between λt values as in equation (3.1), care must be taken to ensure that not only the range of the overall isotopes is covered, but that the difference between the values is also addressed. Using 16 digits of precision, any difference between the two smallest λ values that exceeds 16 orders of magnitude has no effect on the values of the argument vector, \vec{x} . This sets a practical limit to the range of arguments necessary to fully test the calculation routines.

The input values can now be specified for the test problems needed to verify the operation of the exponential moments function subroutines. Values that populate \vec{x} must have values that range between 1.83×10^{-42} and 2.89×10^{44} and cover up to 21 orders of magnitude (providing a buffer beyond the 16 digits of working precision). Additionally, because the exponential moments function routine handles special cases for argument vectors of size of one, two, and three and a general case to break down larger problems into one of these three cases, \vec{x} , need only consist of up to three values to completely exercise all of the calculation paths.

In practice, verifying this section of the code was accomplished by specifying a 1.0 second time step and adjusting the decay constants to the necessary values to

compensate. While not strictly necessary from the point of view of the code, it greatly simplified the input to Mathematica for use in the benchmark calculations.

IV.B: Creating the Calculation Inputs

The input for the decay constants used in the decay calculation routine had to be rational numbers so that Mathematica could perform the calculations with an arbitrary precision to produce the benchmark values. To satisfy the rational number requirements of both applications, I decided to define all decay constant by an integer value. Each integer value was then used as part of an exponent of 10 to generate the necessary values specified previously. The four decay constant values were calculated using the following equations.

$$\begin{aligned}\lambda_1 &= 10^{\frac{i_1}{1001}} \\ \lambda_2 &= 10^{\frac{i_2}{1002}} \\ \lambda_3 &= 10^{\frac{i_3}{1001}} \\ \lambda_4 &= 10^{i_4}\end{aligned}\tag{4.1}$$

IV.C: Verifying the Calculations

Mathematica was chosen to benchmark the results of the exponential moments function routine because it allows a user to specify the number of working digits of precision used in calculating the results. This increased working precision comes at the price of increasing the calculation time significantly. The Mathematica solution was generated by passing in the decay constant values and calculating the answer using the

Bateman solution. The Mathematica notebook used for verification is attached in Appendix C.

A symmetric relative difference (SRD) was used to compare the results from the two methods. The SRD is defined as

$$\delta_{SRD}(y, z) = \begin{cases} 0, & y = z = 0 \\ \frac{|y - z|}{(|y| + |z|)/2}, & \text{else} \end{cases}, \quad (4.2)$$

where y is the result produced by the exponential moments function routine and z is the result produced by Mathematica. I chose to use the SRD as a measure of performance because it is easy to interpret, with a value of 2.0 being the worst case scenario and indicating that the results are uncorrelated between the two methods. Conversely, an SRD close to zero indicates close agreement between the two methods.

I experimented with the working precision of Mathematica during the computation, looking for the fastest computation time that still produced the smallest SRD. I found that only after increasing the working precision to at least 100 digits did the two computational methods converge, producing $\delta_{SRD_{\max}} = 1.0147 * 10^{-11}$. The $\delta_{SRD_{\max}}$ sets a limit on how much disagreement there is between the benchmark and the code calculations. The value indicates that the answer produced by the code is good through at least ten digits. Because no half lives are known with uncertainties to more than five digits, the Monte Carlo propagation of uncertainty reflects only the uncertainties in the half lives and not uncertainty due to calculations in the code.

This worst case scenario was recorded for the following argument set

$$\bar{x} = \begin{pmatrix} 0.147996 \\ 0.147837 \\ 0.147679 \end{pmatrix}. \quad (4.3)$$

Three close together not too small ($x_{smallest} > 0.1$) arguments produced the worst case conditions for the code.

The requirement that Mathematica have at least 100 working digits of precision implies that current methods for computing the decay of radioactive isotopes using the Bateman solution, even if performed using quadruple precision, may not be accurate to the same precision as the double precision exponential moments function solution.

IV.D: Verifying the Depth First Search Routine

The decay chain algorithm uses a recursive subroutine to perform a depth-first search of all daughter products for a given isotope. Testing this algorithm meant creating test problems made up of test isotopes with the necessary decay chain complexity to ensure that any chain that was present in the actual isotope list could be completely described.

The first and most simple problem is the decay from isotope “A” to isotope “B”, $A \rightarrow B$, where A is radioactive and can only decay to isotope B which is stable. From here, the sample chains grow longer (up to 18 isotopes in length) and more complex with an increasing number of branches (the maximum number of branches tested is three). A complete list of the test decay chains is in Appendix B.

Once each isotope list is read in, the depth-first search is called and the decay chains are found. After a chain is completely identified the decay calculation subroutine

is called. The decay constants passed to the calculation subroutine are then compared against a list of the expected decay constants created by hand for each test problem. By this method, every time a decay chain calculation is called, the information is compared to ensure that it is complete and accurate. Any errors in the depth first search are output to the screen so that the user can evaluate the problem.

The depth first search also provides an opportunity for a further test of the exponential moments function, and the results calculated during the depth first search verification are compared again against the Mathematica solution using the SRD.

V. *Monte Carlo Estimation of Uncertainty*

A Monte Carlo simulation was used to quantify the effect of half life uncertainties on the gamma activity produced by neutron induced fission. This was done by using an approximation of a Gaussian distribution of pseudo-random numbers to perturb the half life of each isotope using the uncertainty and then tracking the changes in the quantity of each isotope and the gamma radiation activity as a result. By doing this 1000 times, the effects of the half life uncertainties can begin to be quantified.

Because of the large relative uncertainties in the half lives of the isotopes, the distribution cannot in fact be Gaussian. A truly Gaussian distribution requires an infinite number of standard deviations from the mean to cover all possible outcomes. For real world data, a Gaussian approximation may be appropriate if a reasonable (3σ) distribution of the data encompasses nearly every possibility. However, with the data provided, some isotopes have standard deviations which are large compared to the half life (see Table 1) and predict negative half lives within the 3σ tolerance.

Recognizing that calling the half life uncertainty a standard deviation does not adequately describe the data, I chose to treat the distribution as Gaussian and use rejection and re-sampling to ensure that every half life has a positive value. Clearly this approach only provides a first cut at quantifying the uncertainty in the activity calculations, but this should still be sufficient to gain a better understanding of how the uncertainties are propagated through decay chains.

An approximation to a normal distribution of random numbers was created by taking the sum of twelve pseudo-random numbers uniformly distributed between 0 and 1

and subtracting 6.0. This method provides a good approximation to a normal distribution near the center, but loses fidelity at the tails of the distribution. For the purposes of this thesis, the behavior at the middle of the distribution was the important component and this method models the normal distribution well enough for tracking the propagation of uncertainty in the isotope data.

Once the random number is produced, the value was then multiplied by the uncertainty in the half life and added to or subtracted from the half life. If a non-positive value for the half life is obtained by this method, another random variable is chosen until a positive half life is found. Random variables were chosen using the built in random number generator in Compaq Visual Fortran[2].

VI. Performance, Results, and Analysis

The implemented exponential moments function code combined with the use of a transmutation matrix is faster than the differential equation solver or the Bateman solution with the specified digits of working precision in Mathematica. Moreover, the code produces answers that are more precise than other methods using the same digits of precision. The rest of this chapter will outline the performance of the code as well as show results from the fission product test problems.

VI.A: Performance

The time it takes to produce $N(t)$ and $A(t)$ with the code is highly dependent upon the time of interest. The overhead of reading in the decay data to populate $\bar{N}(0)$ values and gamma data must be performed only once with each data set. Then the populated data arrays are stored to the hard drive in binary format for quick processing during future runs.

The major factor in the run time of the code is the production of the T-matrices. Once a T-matrix is generated, it is saved to the hard disk in a sparse format for future use which greatly speeds any subsequent calculations using the same time of interest. The time required to create a T-matrix from scratch depends on the time of interest.

At very short times, nearly all arguments passed to the Fortran routine are small. When this is the case, series expansions are used which are calculated quickly in Fortran. For very long times, arguments to the exponential moments function all become larger than 38.0 and the T-matrix is generated quickly at these times as well. However, for time steps where many of the arguments passed to the exponential moments function are

neither all large nor all small, calculating the results becomes computationally costly as the number of EXP() calls reaches a maximum.

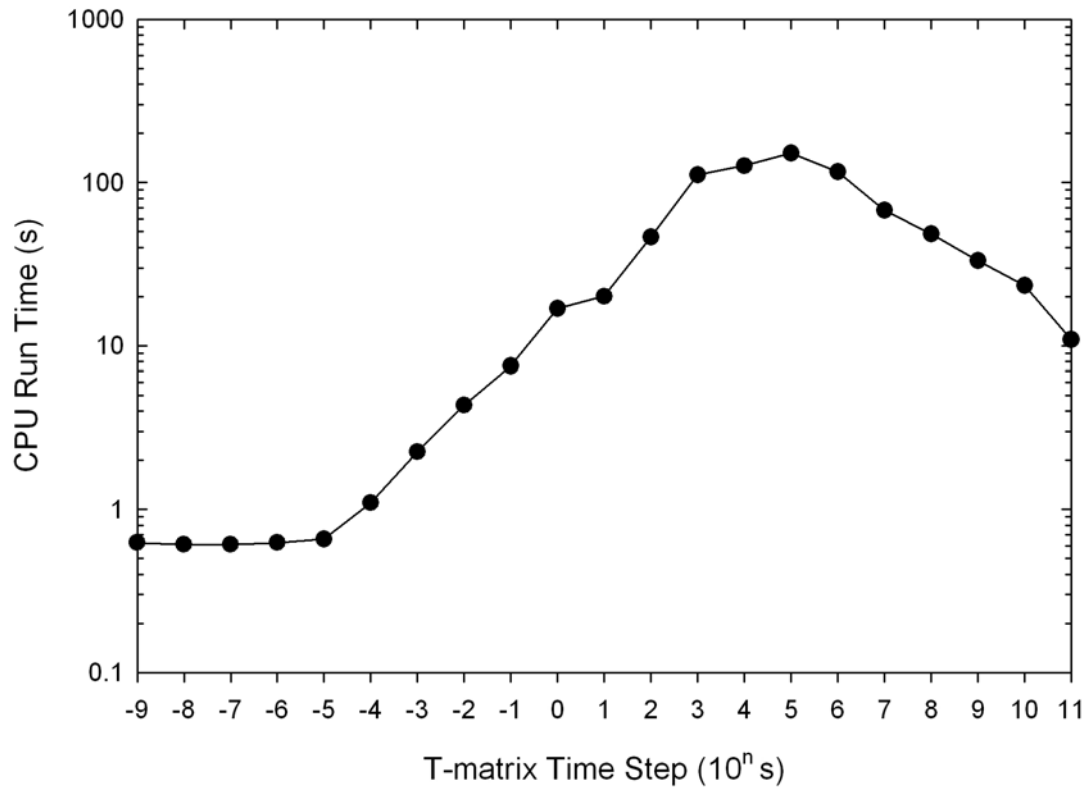


Figure 7 Time to Generate T-matrix for Given Time Steps

The computer used to execute the code had a 2.8 GHz Pentium D processor (a dual core chip running the code on only one of the processors). However, for longer time steps, it becomes more advantageous for the user to use stored T-matrices to reduce the run time. For this reason, a newly generated T-matrix is automatically saved in a sparse format once it is created.

These results are indicative of the computational cost for the current algorithm which is only optimized to preserve precision. Optimizing the exponential moments

function module for speed with long argument vectors should result in significant reductions in computer run time.

VI.B: $A(E,t)$

I arbitrarily used 11 different gamma energy bins to sort the output of the decay code. One energy bin covered all gamma energies, while the remaining ten each covered a 1 MeV span without overlap between 1 MeV and 11 MeV. The gamma activity varied greatly from the freshly irradiated fuel state 1.0 nanosecond after irradiation to the last calculated time step of just over 25,000 years.

The plots of total activity show the overall effect of the combination of a fuel and a specific neutron energy spectrum. As is shown in Figure 8, the total activity is dominated by the lower energy gammas. Therefore, the activity at higher energy bins must be examined separately to completely understand the decay process.

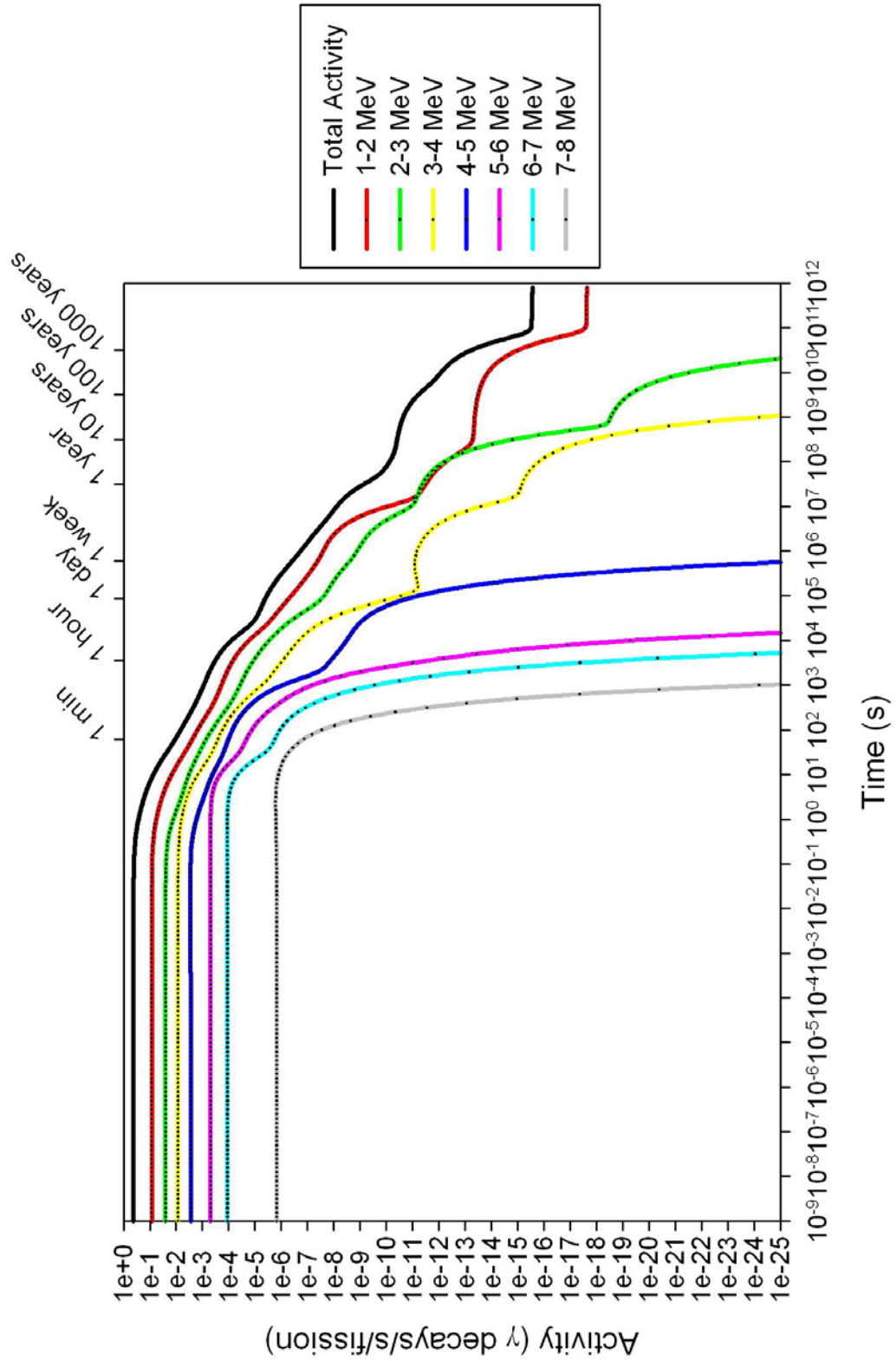


Figure 8 Energy Bin Contributions to Activity for U-235 Thermal

Because of the large ranges of time and activity involved, the most useful way of looking at this data is to break it into two separate sections: an early time which starts at a nanosecond and ends around 10 seconds, and a late time for all times after 10 seconds. Also, by changing the axis scaling, different features of the activity curves are highlighted and examined in greater detail.

1. Total Activity

At times shortly after irradiation the type of fuel profoundly affects the overall activity. U-238 shows significantly more activity than U-235, which is more active than Pu-239. The activity from the fission of Pu-239 with a thermal neutron spectrum so closely matches the activity of Pu-239 exposed to the fast fission spectrum that the lines are nearly indistinguishable in Figure 9.

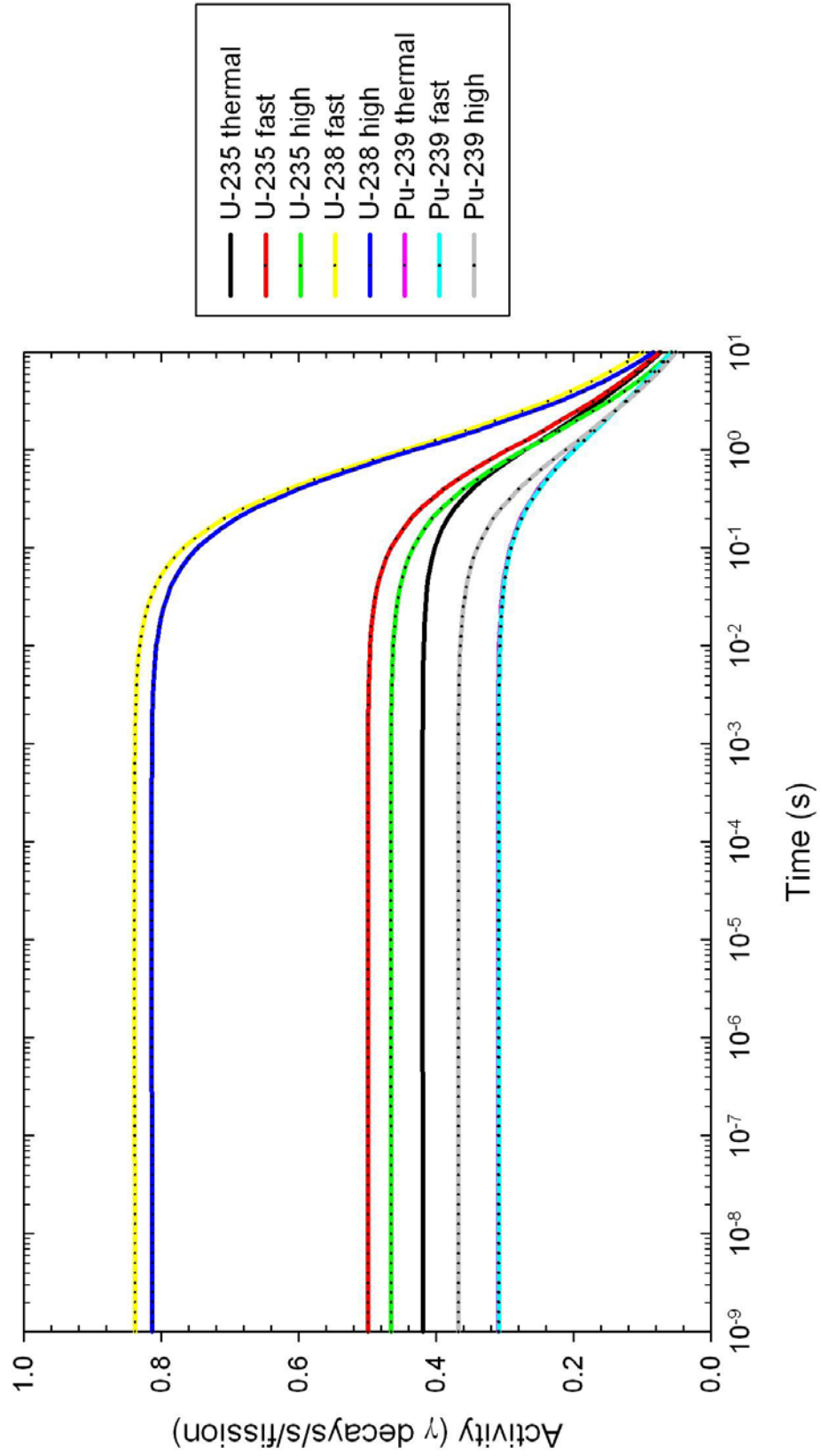


Figure 9 Total Activity, 1 nanosecond to 10 seconds, Log-Linear

As shown above, the activity holds nearly constant until around one tenth of a second. The flatness of the curves is due to only very minor changes in activity at these time steps. This indicates that the process is dominated by either isotopes that have half lives on the order of a tenth of a second up to a few seconds or the isotopes are in secular equilibrium with a parent isotope that has a half life in that same range . Figure 10 shows this finding more directly by using a semi log plot. On the semi-log axis configuration, the plot of activity of a single isotope is represented as a straight line proportional in slope to the decay constant of the isotope. The curves shown in Figure 10 are not perfectly straight because the activities are made up of many isotopes. Each of the top five contributors to the total activity is from isotopes with half lives between 0.2 seconds (Rb-96) and 2.1 seconds (Zr-99), as is shown in

Table 4.

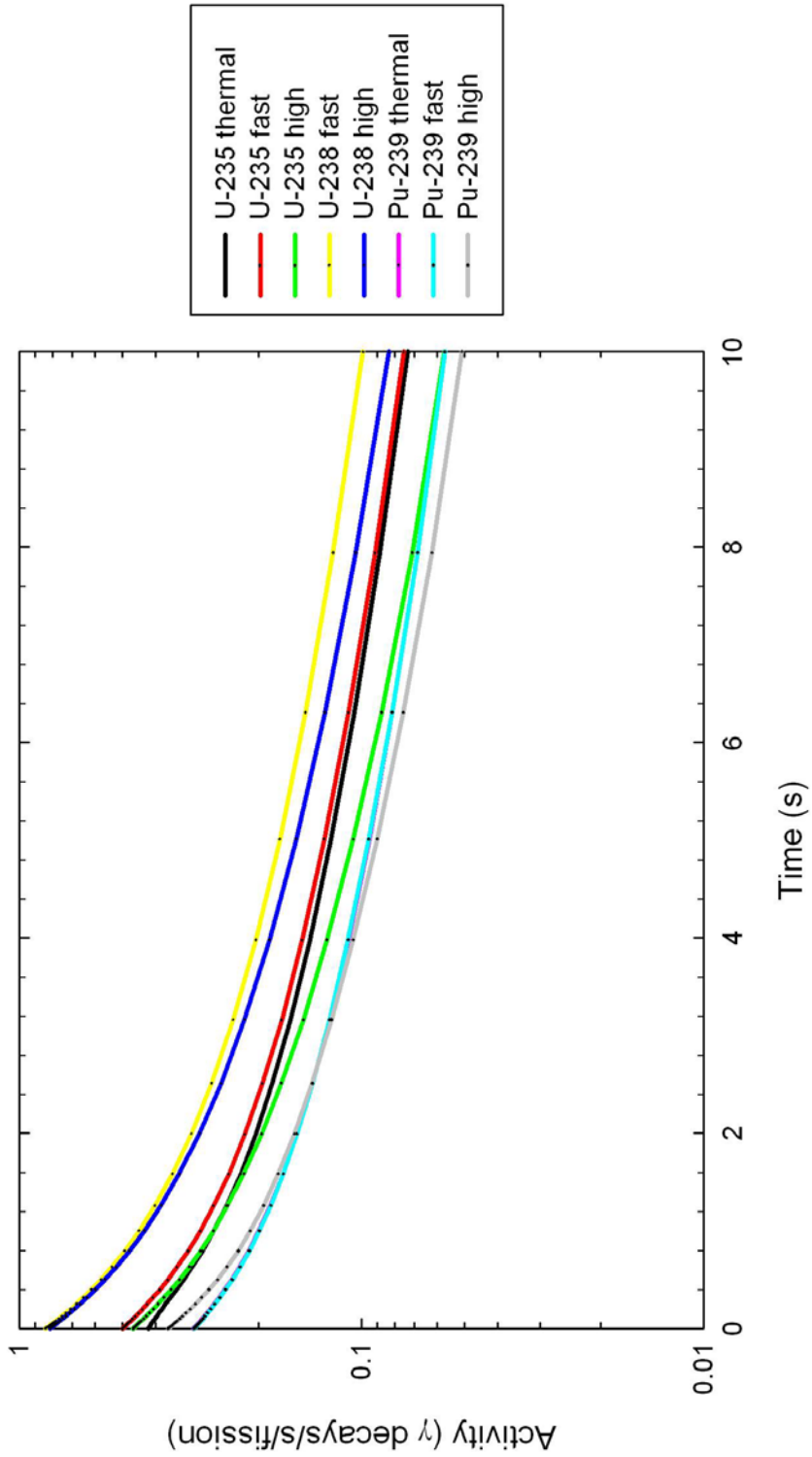


Figure 10 Total Activity, 1 nanosecond to 10 seconds, Semi-Log

Table 4 Major Contributors to Total Activity at 4.64×10^{-5} s and Half Lives

Fuel	Incident Neutron Energy	Primary Contributors	Half Life	
U-235	Thermal	Sr-96	1.07 s	
		Y-98	0.548 s	
		Sr-97	0.429 s	
	Fast	Sr-96	1.07 s	
		Y-98	0.548 s	
	High	Y-98	0.548 s	
		Xe-134m	0.290 s	
U-238	Fast	Sr-96	1.07 s	
		Rb-96	0.2028 s	
		Y-100	0.735 s	
		Sr-98	0.653 s	
	High	Sr-96	1.07 s	
		Y-98	0.548 s	
		Rb-96	0.2028 s	
		Y-100	0.735 s	
	Pu-239	Fast	Sr-96	1.07 s
			Y-98	0.548 s
Zr-99			2.1 s	
High		Xe-134m	0.290 s	
		Y-98	0.548 s	

Figure 11 shows a semi-log plot of the total time to show that the activity curves at late times are each very similar in slope. The flatness of the activity curves at the end of the calculation range is due to the same isotope in each fuel, Sb-126. The half life of Sb-126 is only 12.35 days. Here Sb-126 is in secular equilibrium with Sn-126 which has a half life of 230,000 years. The activity due to the decay of Sb-126 accounts for more than 90% of the total gamma activity in each decay chain. The differences in the activity between isotopes reflect the initial allocation of fission fragments by mass number. High energy neutrons create fission products with a mass number of 126 with more frequency than fissions induced by neutrons of lower energy. The correlation of this relationship between the production of fission products with atomic numbers of 126 and the activity at 25,000 years is 0.992.

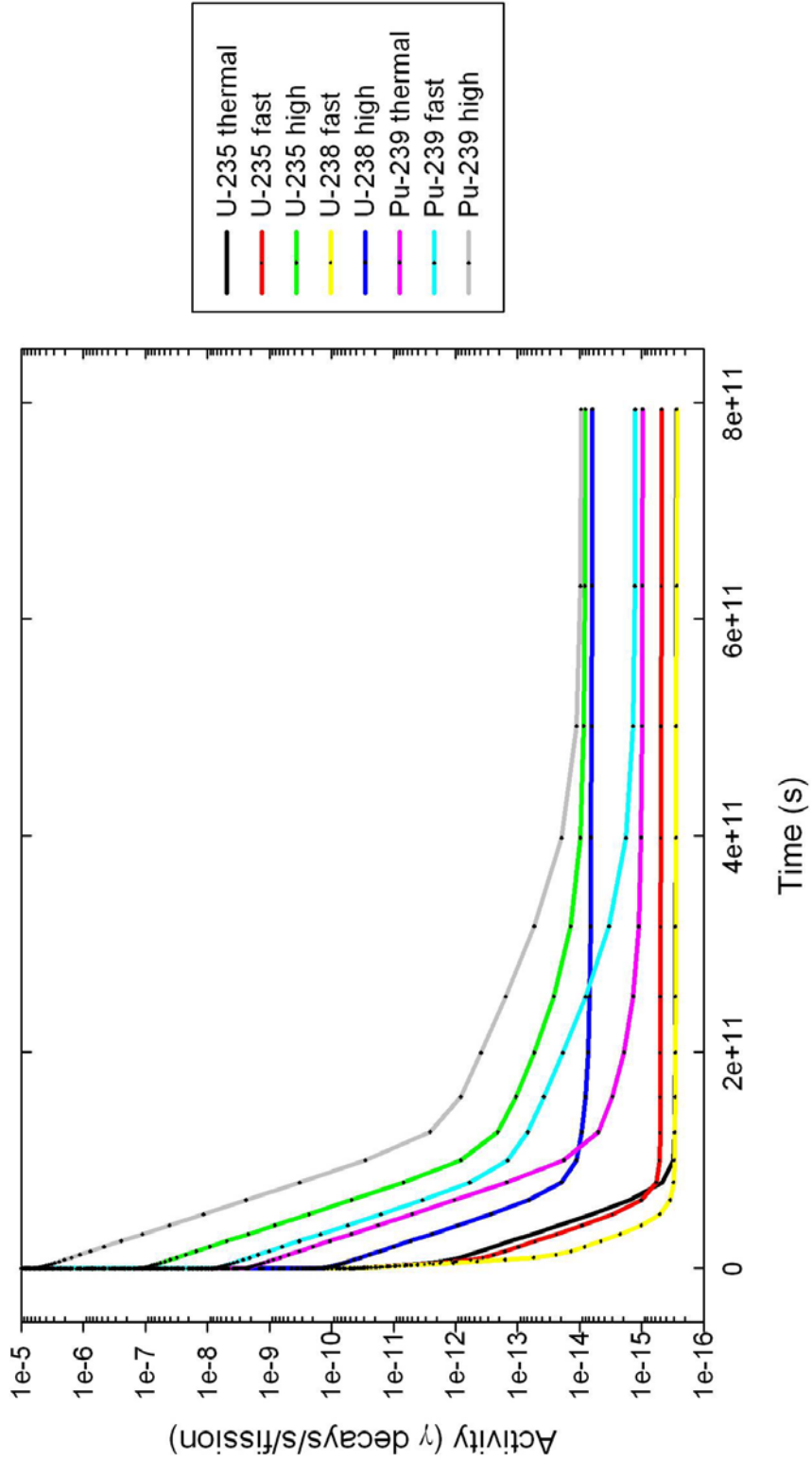


Figure 11 Total Activity, 1 nanosecond to 25,000 years, Semi-Log

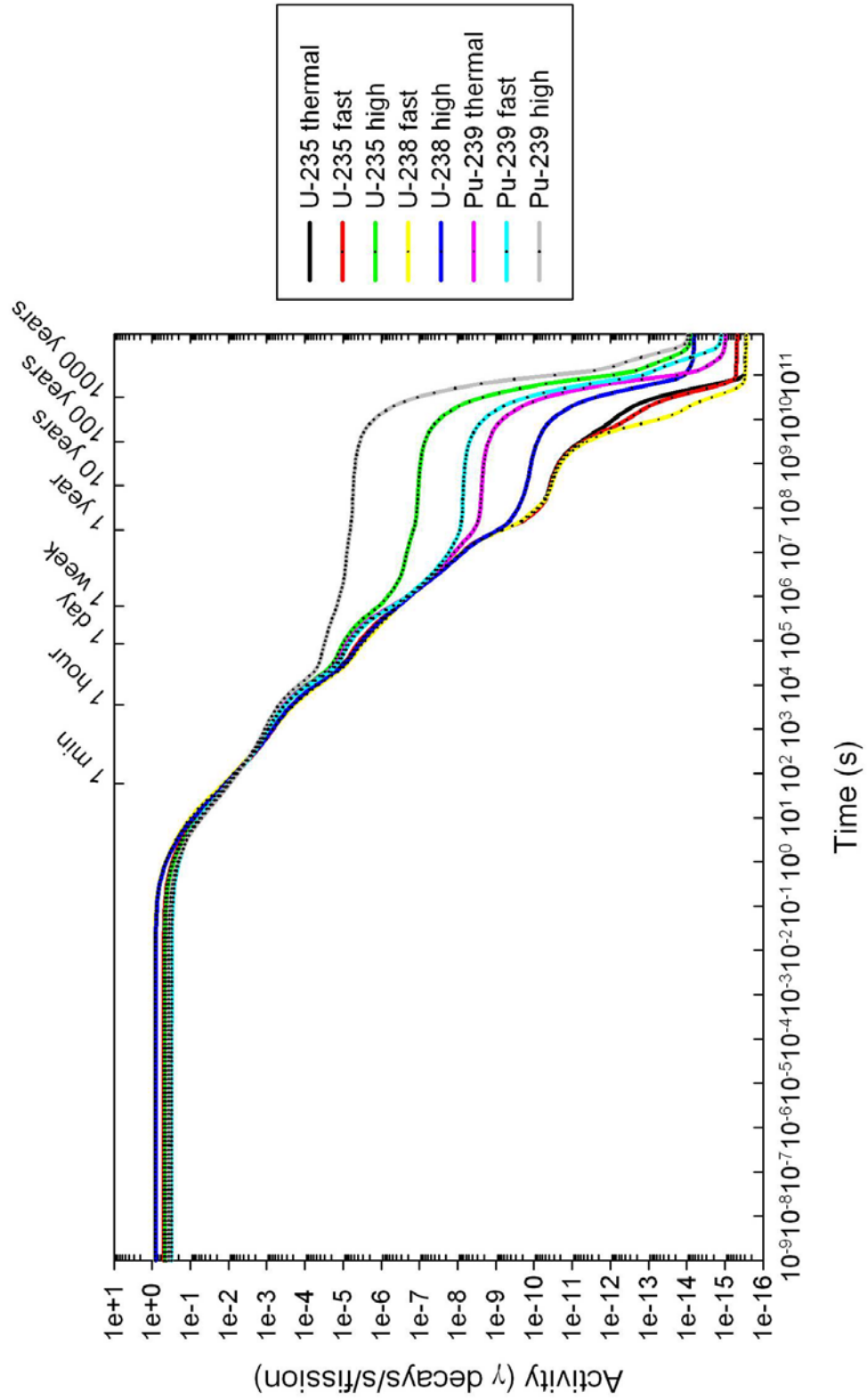


Figure 12 Total Activity, 1 ns to 25000 years, Log-Log

Figure 12 uses logarithmic axes to show detail in the activity curves over the time of interest. Here we see that the activities are due to a combination of fuel and incident neutron energy. For each fuel, the activity is highest for the D-T neutrons by several orders of magnitude. For the same incident energy neutrons, the fuels are Pu-239, U-235, and U-238 in order of decreasing activity. The areas of the curve that are largely flat are not completely straight due to many small contributions by isotopes with half lives of the same order of magnitude as the time in question. The portions of the curves with large slopes indicate times where the magnitude of the half lives of the principal contributors to the activity are of the same order of magnitude as the time. For example, at the one year point, the principal contributor to the total activity for plutonium and the high energy neutron fission of U-235 is Tb-158 with a half life of 180 years. The remaining fuels (U-235 thermal, U-235 fast, U-238 fast, and U-238 high) have nearly the same change in activity at the one year point due to the same two primary contributors, Nb-95 (half life of 34.991 days) and Zr-95 (64.0 day half life), which together account for more than 75% of the total activity in these fuels. This explains why four of the curves are basically flat and four have large slopes at 1.0 year in the graph above.

Figure 13 shows plots of the gamma power (the product of activity and the gamma energy) with respect to time for each fuel and neutron spectra. Additionally, the plot overlays the Way-Wigner approximation of $t^{-1.2}$. This clearly highlights the poor approximation of the actual dose rate, especially for the D-T neutron fission of Pu-239.

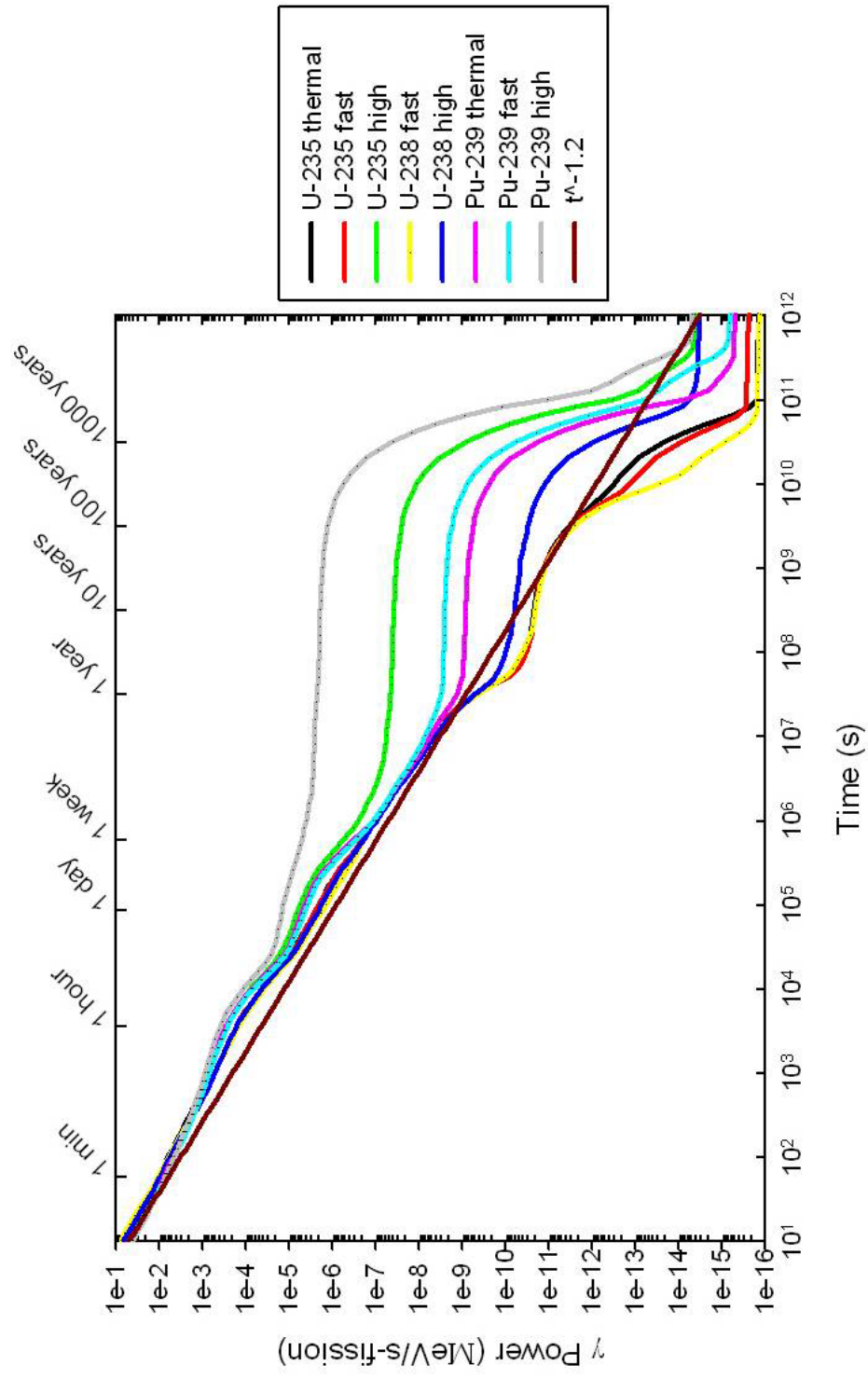


Figure 13 Gamma Power and the Way-Wigner Approximation

2. 1-2 MeV

The plot of short-time gamma activity in Figure 14 closely resembles the shape of the total activity curves in Figure 9. The 1-2 MeV gammas account for approximately only one fourth of the total activity. As in Figure 9, Figure 14 shows that the early time activities are more dependent on fuel than neutron energy, although the Pu-239 high energy fission curve is now nearly indistinguishable from the U-235 thermal curve.

Once again, the list of major contributors to the 1-2 MeV activity bin shows that all have half lives in the several tenths of a second to a few seconds which corresponds well to the roll over of all of the curves that occurs somewhere after 0.1 seconds. The nearly straight curves in the semi-log plot shown in Figure 15 shows that the activities of each of the fuels is caused by multiple isotopes, each with similar half lives. The near-parallel nature of the curves indicates that the mixes of isotopes from each fuel sample are likely to have many of the same daughters.

Figure 16 shows the entire range of calculated data. Once again, this plot closely matches the plot of the total gamma activity. The steep slope at early times shows nearly parallel lines. The activity in this bin at 2.5×10^{10} seconds (approximately 800 years) is primarily due to the decay of Tb-158 (180 year half life). Activity at the end of the time of interest is dominated by the decay of Sb-126, just as was the case for the total activity.

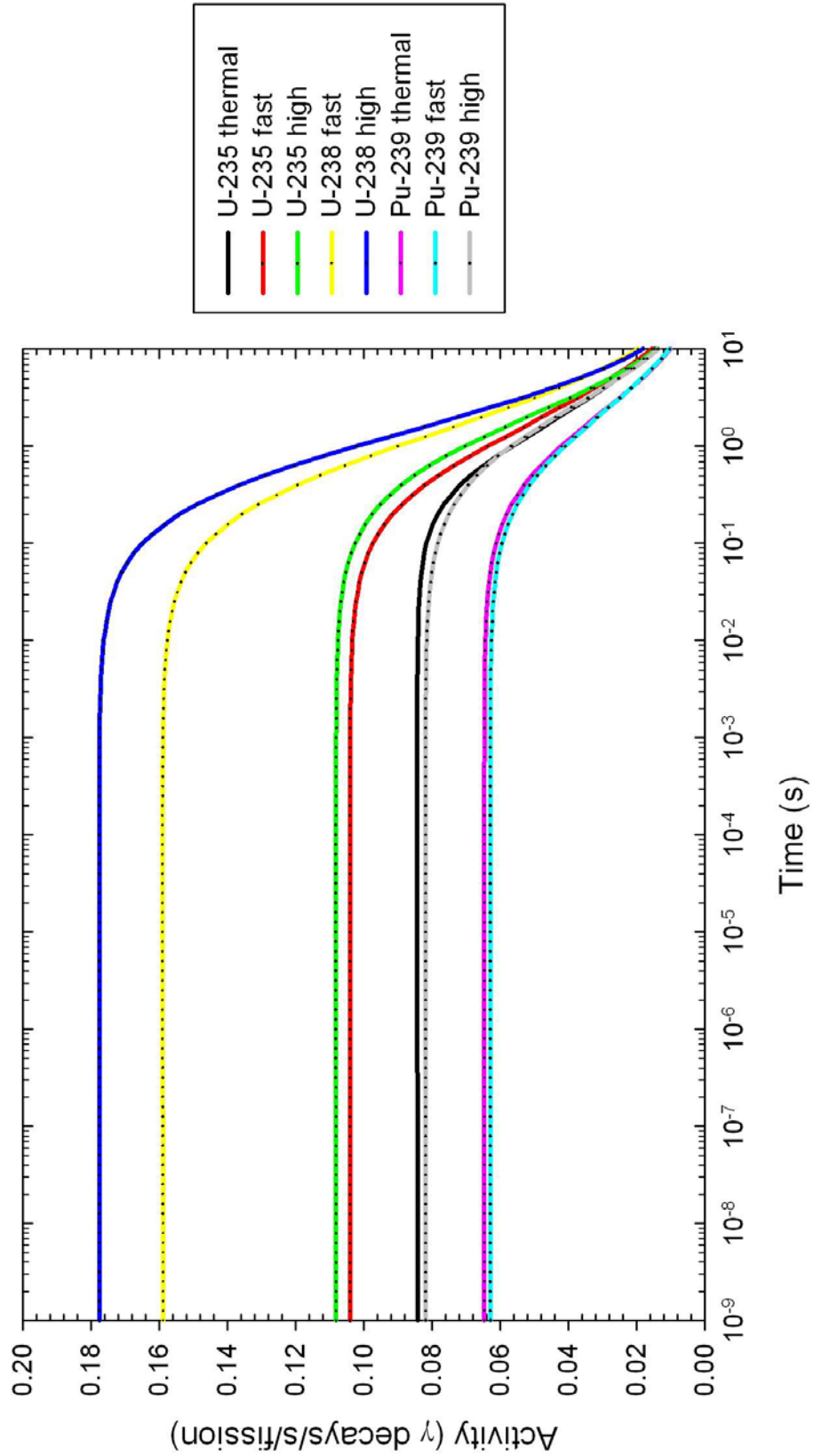


Figure 14 Activity, 1-2 MeV Gammas, 1 ns to 10 s, Log-Linear

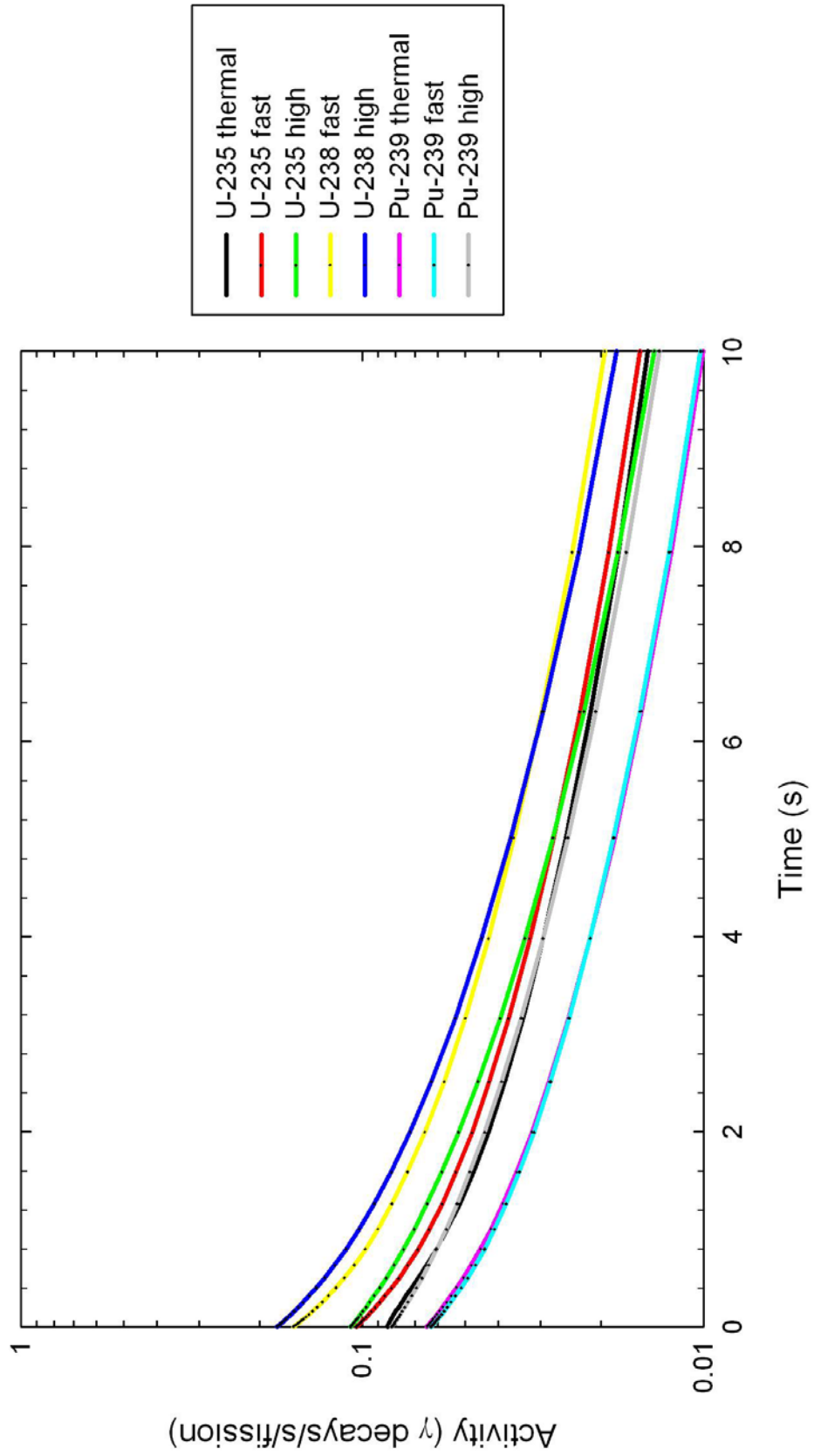


Figure 15 Activity, 1-2 MeV Gammas, 1 ns to 10 s, Semi-Log

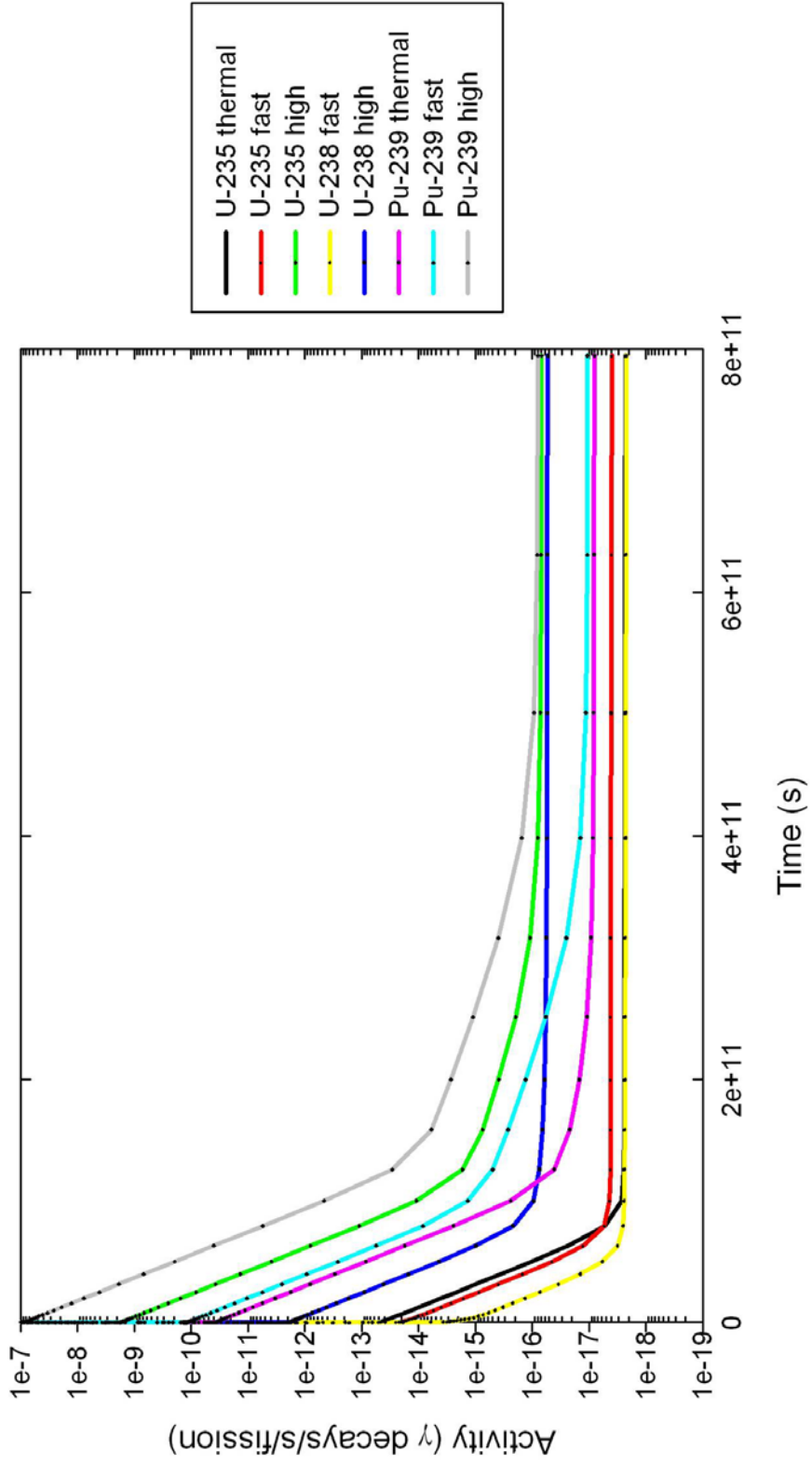


Figure 16 Activity, 1-2 MeV, 1 ns to 25,000 y, Semi-Log

3. 2-3 MeV

During times up to 10 seconds after irradiation of the fuel source, the activity curves once again closely follow the shape of the 1-2 MeV activity, as well as the total activity. However, as the bins continue to increase in energy, there is a decrease in the magnitude of the activity in each bin. Whereas the 1-2 MeV accounted for approximately one fourth of the total activity, the 2-3 MeV gammas only account for around a tenth of the total activity. The curves shown in Figure 17 show the 2-3 MeV gamma activity curves. The graph shows that the difference in fuel source is even more pronounced in this energy bin. Sr-97 and Y-98 are the significant contributors for each fuel and fission neutron energy in the 2-3 MeV energy bin.

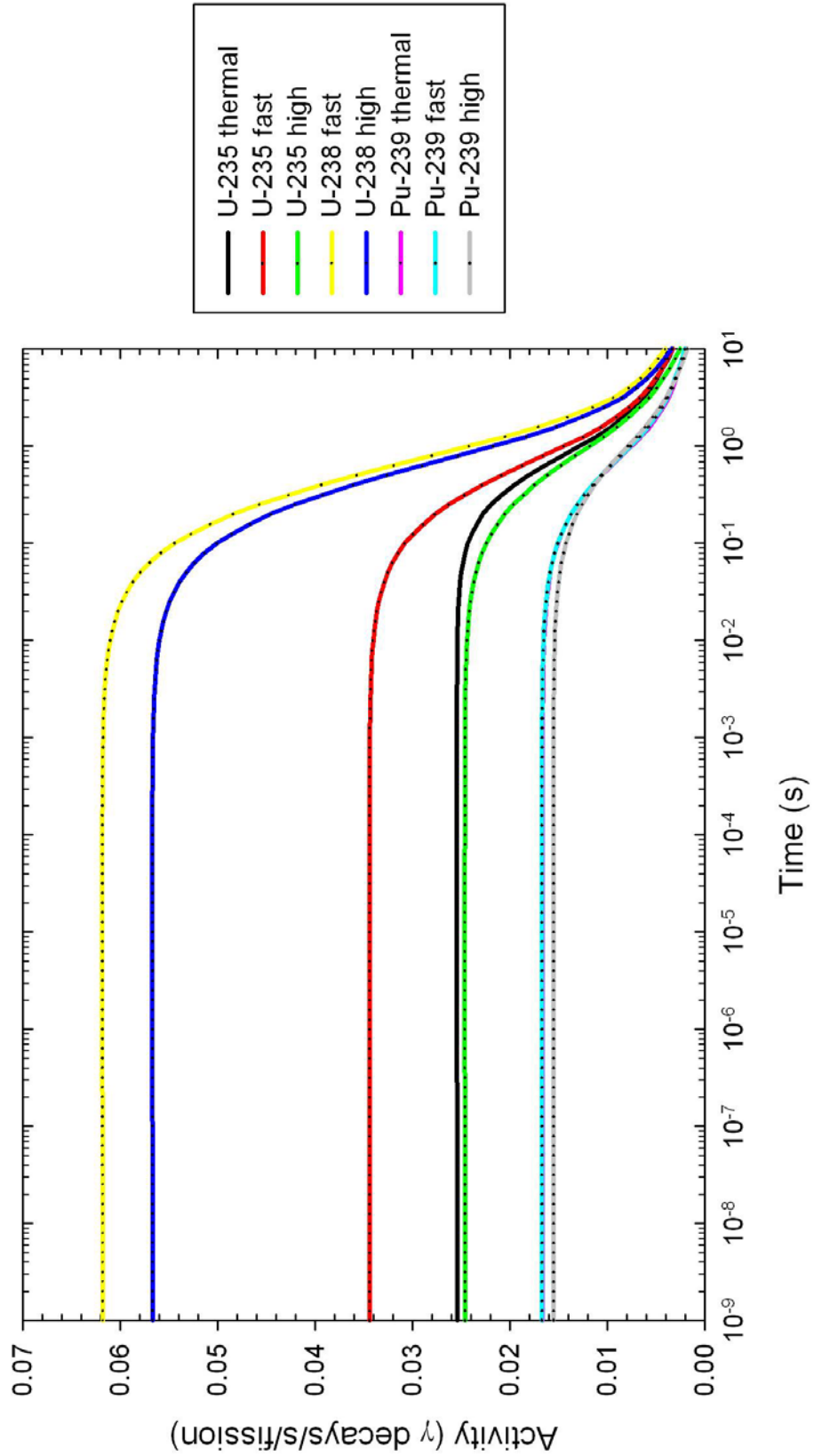


Figure 17 Gamma Activity, 2-3 MeV, 1 ns to 10 s, Log-Linear

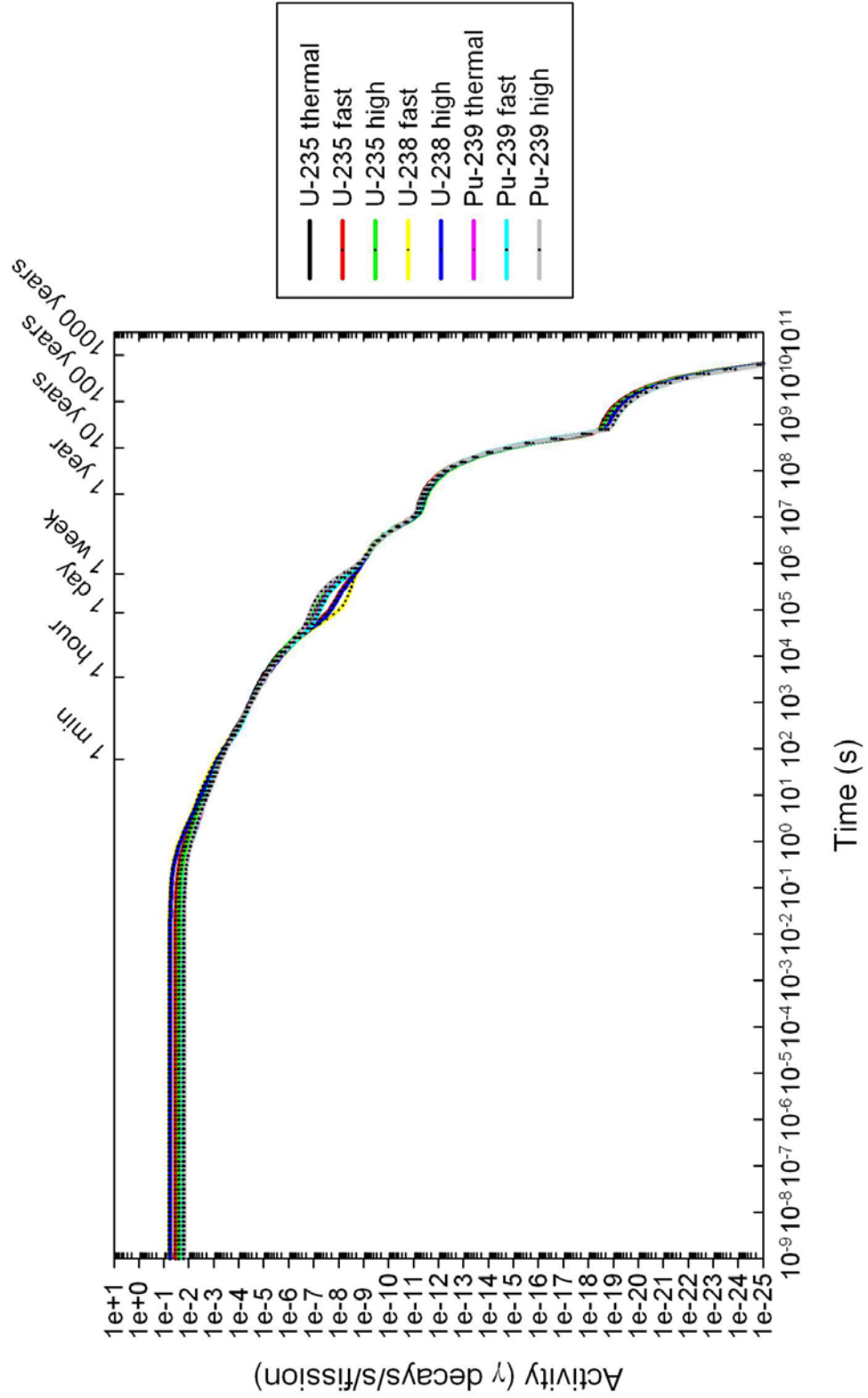


Figure 18 Gamma Activity, 2-3 MeV, 10 s to 25000 y, Log-Log

Figure 18 shows the gamma activity in the 2-3 MeV energy bin for all times of interest. This is the first gamma energy bin for which the activity drops below an intensity of 10^{-25} gamma decays per second per fission before the simulation was completed. I have set this as a lower threshold for all graphs to facilitate comparisons among the plots. In all cases, the slope is nearly vertical when the curve crosses this threshold, and there are no defining characteristics below this threshold.

Figure 18 also shows that activities for all fuel sources and incident neutron energies are nearly indistinguishable, with the exception of the sub 1.0 second activities shown in Figure 17 and a separation in the activities between 10^5 and 10^6 seconds. This second area is magnified in Figure 19.

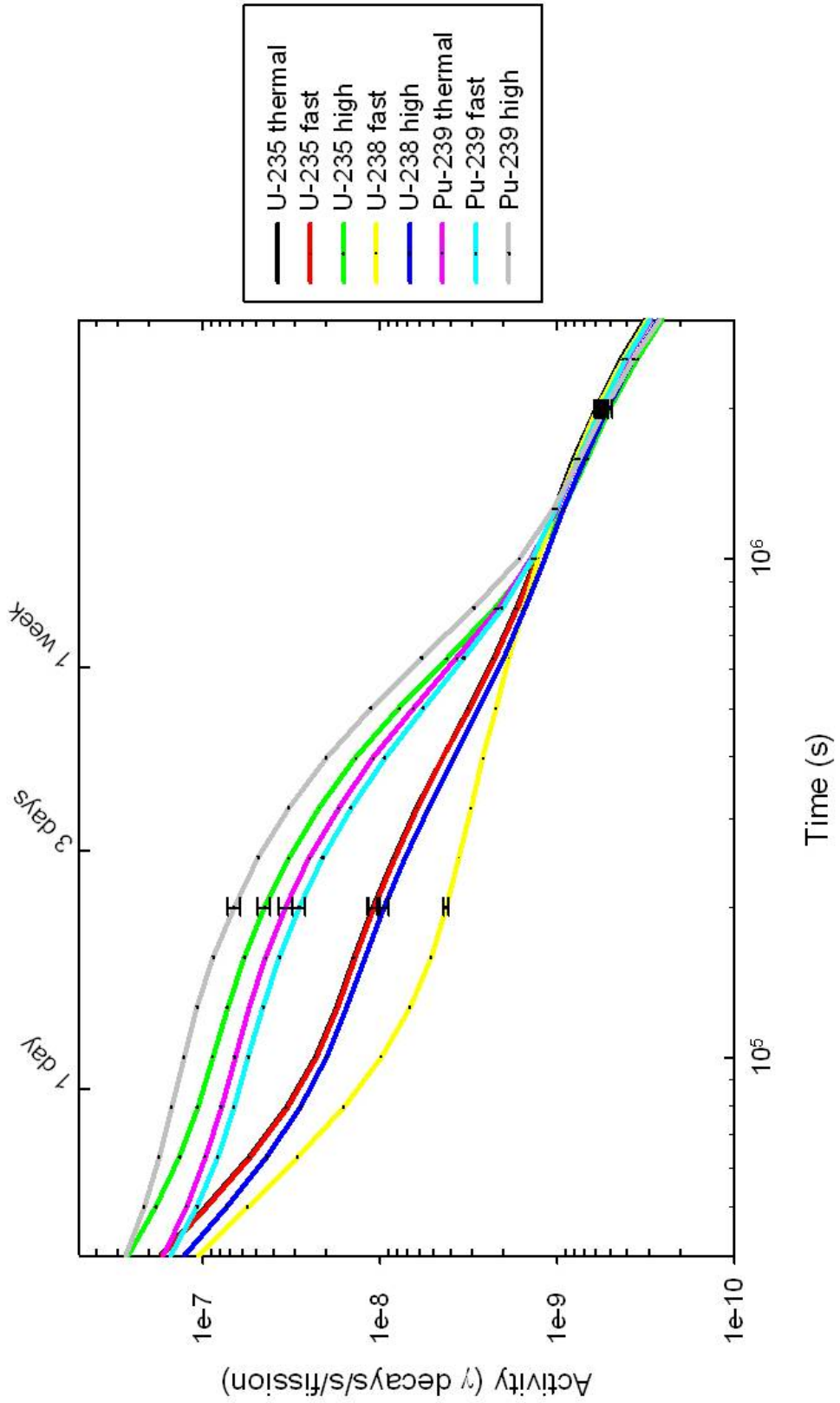


Figure 19 Gamma Activity with Uncertainty, 2-3 MeV, 1 day to 3 weeks

The uncertainty bars in Figure 19 are standard deviations for a normal distribution of the activity over 1000 test runs. The activity results were each checked for normality using the Kolmogorov-Smirnov test. The standard deviations show that the fuels are largely distinguishable within 1σ after approximately two days of decay time, but that after approximately three weeks, all of the curves are statistically indistinguishable.

The activity curves for U-235 with fast and thermal neutrons are nearly indistinguishable, however the rest of the fuels and neutron sources show up to almost two orders of magnitude difference. At 10^4 seconds (2.8 hours), different sources each have the same major contributors to the total activity, albeit in varying intensities. The main isotopes at this time are: Kr-88 ($t_{half} = 2.84$ days), Cs-138 ($t_{half} = 33.41$ minutes), La-142 ($t_{half} = 91.1$ minutes). Each of these isotopes is effectively gone by one week and the activity becomes dominated by isotopes from new mass chains. At $2 \cdot 10^5$ seconds (2.3 days), the primary contributors to the activity become dominated by the metastable state of Te-131 ($t_{half} = 1.35$ days), I-132 ($t_{half} = 2.30$ hours), and La-140 ($t_{half} = 1.68$ days). The I-132 activity is produced following the decay of Te-132 ($t_{half} = 3.26$ days). After 3 weeks, the activities from each graph join again. At this point, the transition is complete and more than 90% of the activity is caused by La-140 in each isotope. During the period of interest above, the La-140 decay was largely the result of the isotope being produced directly from fission. At later times, it is in secular equilibrium with its parent, Ba-140 ($t_{half} = 12.75$ days).

4. 3-4 MeV

Activities in the 3-4 MeV energy bin only contribute about 2% of the total activity at early times as shown in Figure 20. The separate fuels are once again readily identifiable. At 1.0 second into the decay, the activity is dominated by Y-97 for all test cases.

Figure 21 depicts an activity drop below the 10^{-25} activity threshold at approximately 31.8 years (10^9 s) after fuel irradiation. For times longer than 10.0 seconds, the curves from each input problem closely resemble each other with the exception of some separation around the one year (3.15×10^7 s) point. This separation is more clearly shown with a semi-log plot of the data as in Figure 22. The straight, parallel lines are a reflection that all of the activity at long times is caused by the same isotope, Rh-106 ($t_{half} = 28.9$ s). Rh-106 is in secular equilibrium with its parent isotope, Ru-106 ($t_{half} = 1.02$ years). There is a 99.9% correlation between the total quantity of initial fission products with a mass number equal to 106 and the ratio of the activities shown in Figure 22.

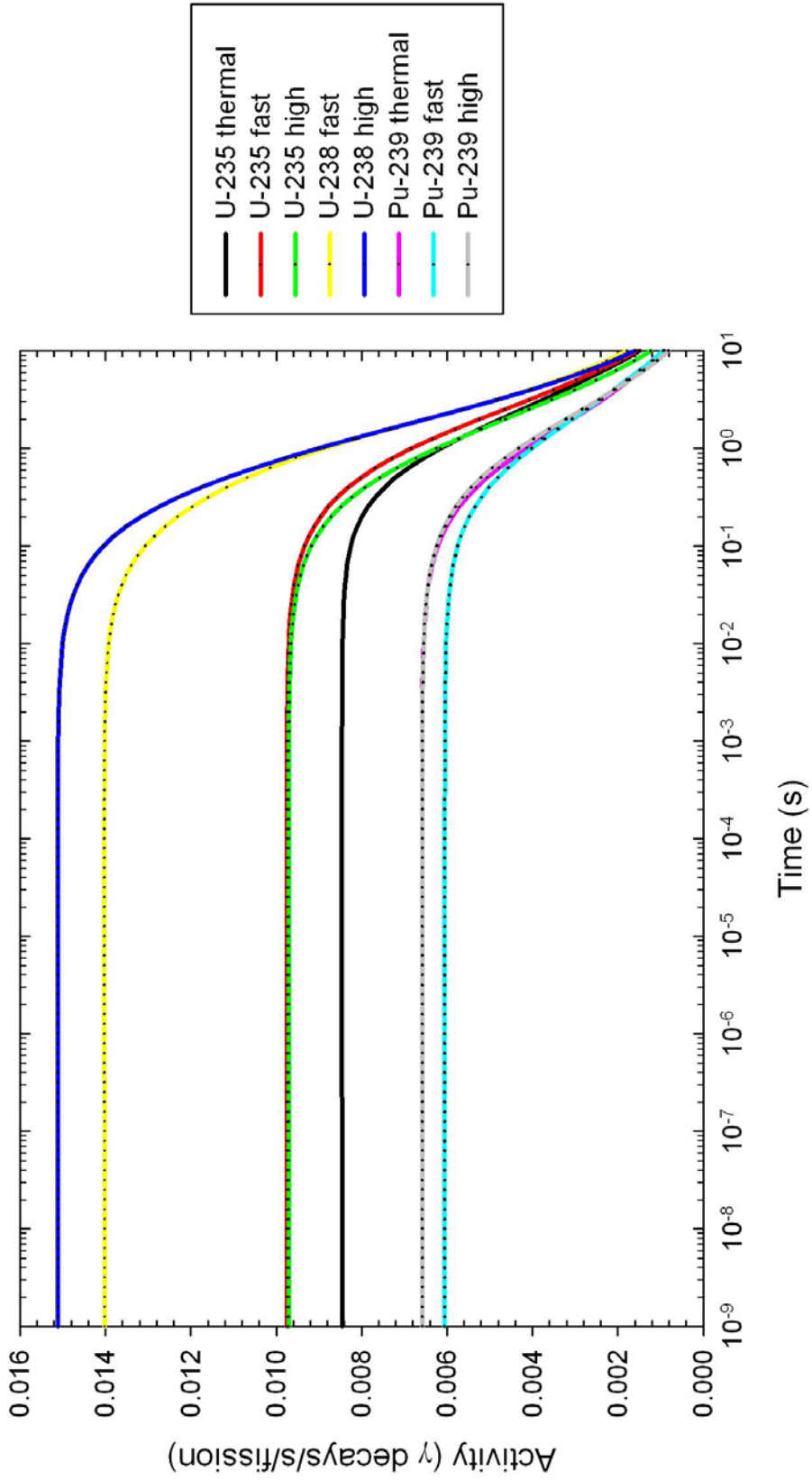


Figure 20 Gamma Activity, 3-4 MeV, 1 ns to 10 s, Log-Linear

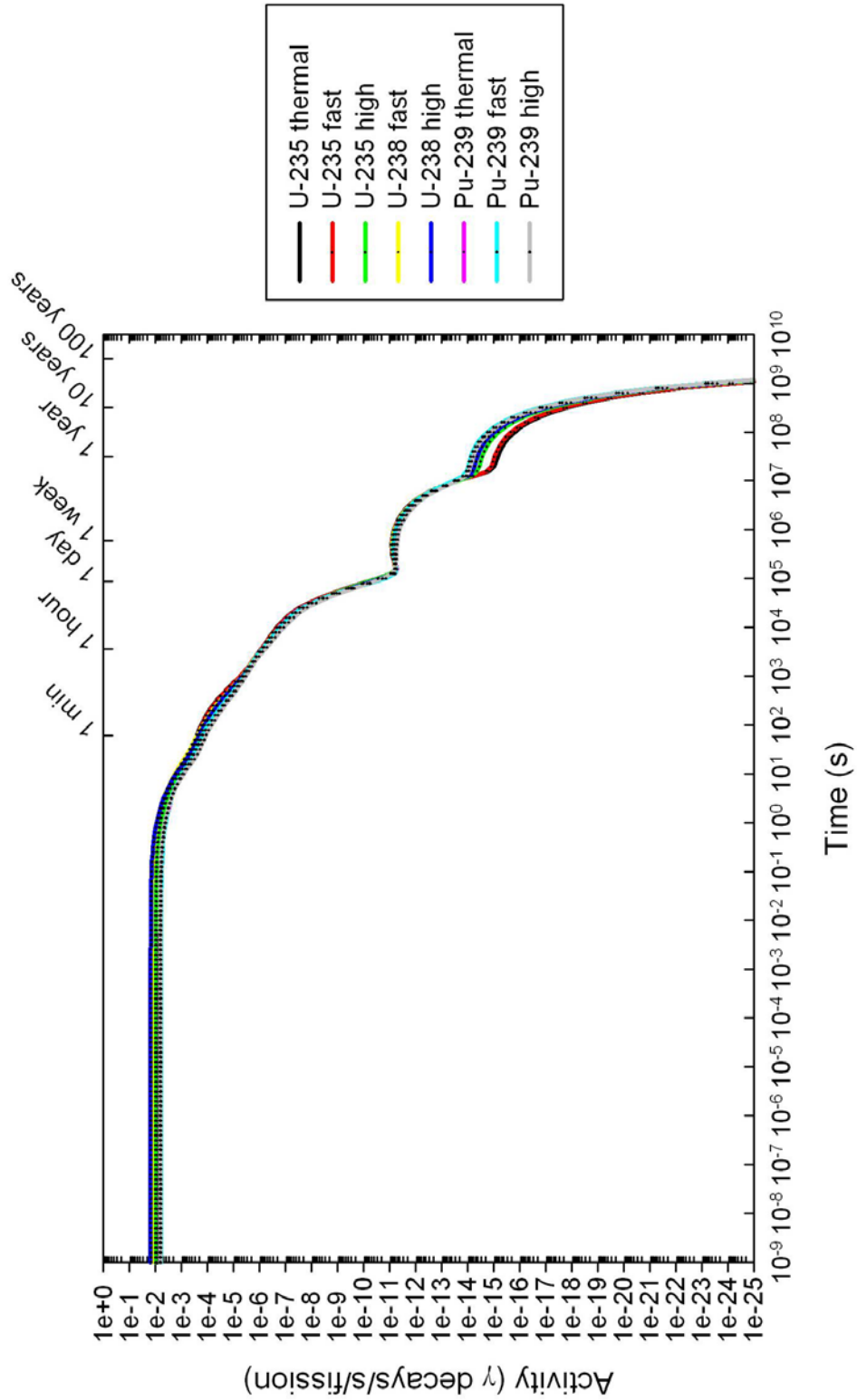


Figure 21 Gamma Activity, 3-4 MeV, 1 ns to 100 y, Log-Log

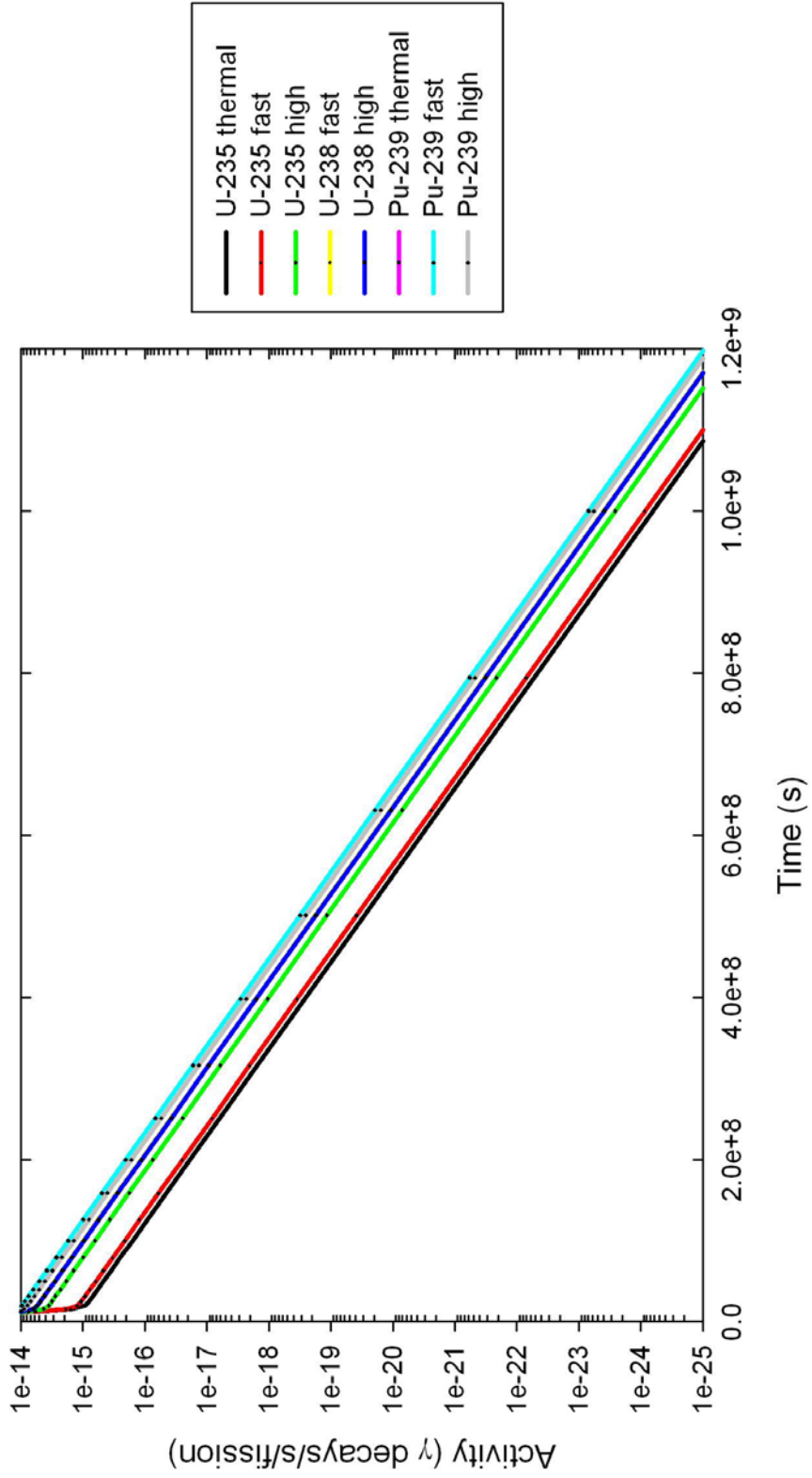


Figure 22 Gamma Activity, 3-4 MeV, 1 ns to 100 y, Semi-Log

5. 4-5 MeV

The activity due to gamma radiations with energies between 4 MeV and 5 MeV continues the trend of decreasing contribution to the total activity, as is shown in Figure 23. The crossing of some of the activity curves is shown clearly in Figure 24 in a semi-log plot. Crossing activity curves for a fission product decay problem indicates that the new activity comes from not just a new set of isotopes, but that the activity from a new mass chain has become predominant.

Figure 25 shows the late time activity of the different fuel sources. At approximately 5.3 days (4.6×10^5 s) after irradiation with high energy neutrons, the Pu-239 source shows a departure from the curves of the other seven test scenarios.

This effect is shown more prominently on a semi-log plot as in Figure 26. The different slopes indicate a difference in isotopes that contribute to the activities. Inspection of the data show that the activity curves of all of the isotopes, except Pu-239 high, are more than 99.99% made by the decays of Rb-88 ($t_{half} = 17.73$ minutes). The relatively short half life of Rb-88 accounts for the very low activities present.

Fission products are typically neutron heavy isotopes that under go beta decays. However, the fission of a Pu-239 nucleus with a high energy neutron results in the production of Ga-66 ($t_{half} = 9.49$ hours), a neutron light isotope that undergoes an electron capture decay. Ga-66 is only produced on average at a rate of 2.02×10^{-14} atoms per fission of Pu-239 by a high energy neutron but produces enough high energy gammas to be significant as the activity from other fission products decays away.

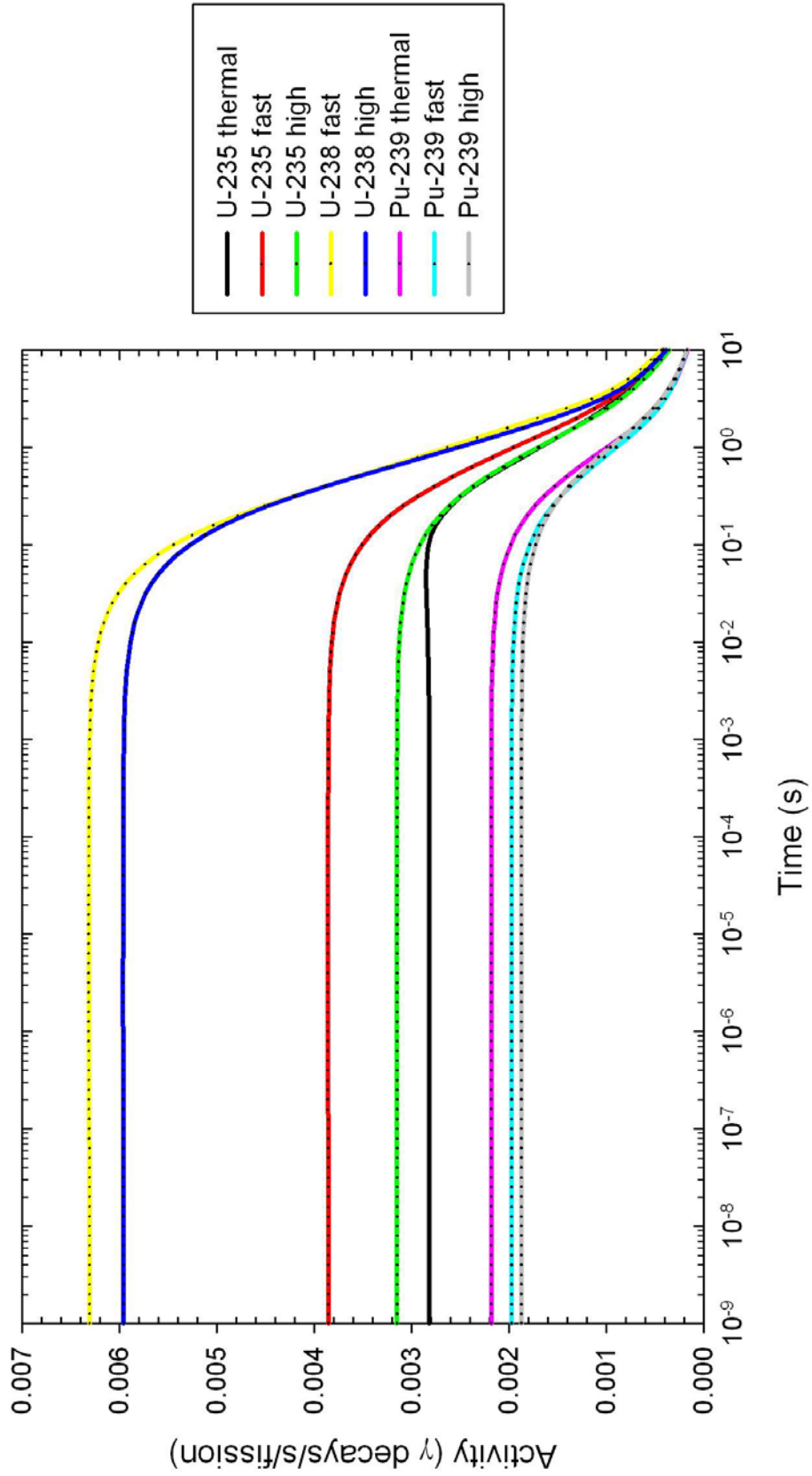


Figure 23 Gamma Activity, 4-5 MeV, 1 ns to 10 s, Log-Linear

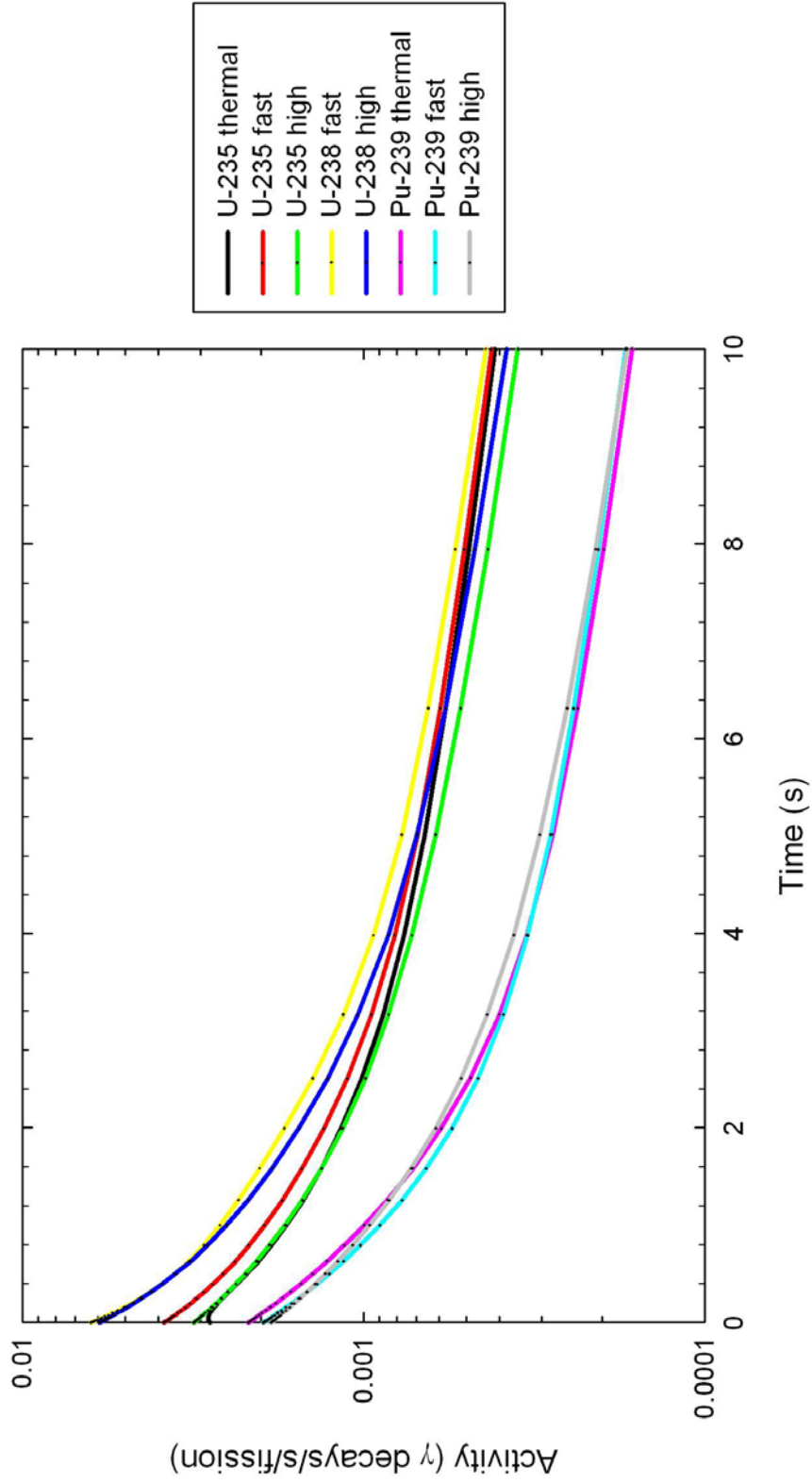


Figure 24 Gamma Activity, 4-5 MeV, 1 ns to 10 s, Semi-Log

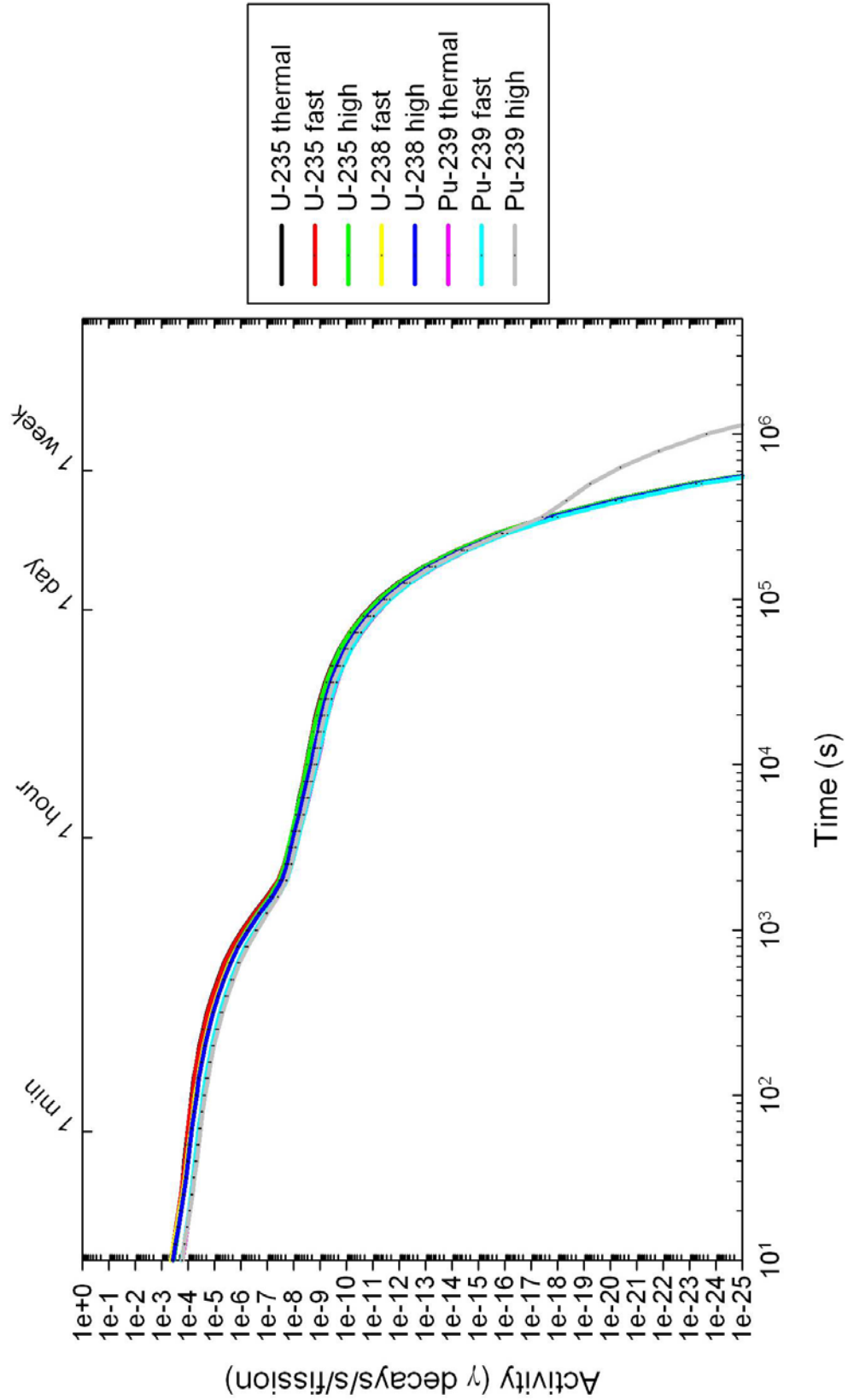


Figure 25 Gamma Activity, 4-5 MeV, 10 s to 10^6 s, Log-Log

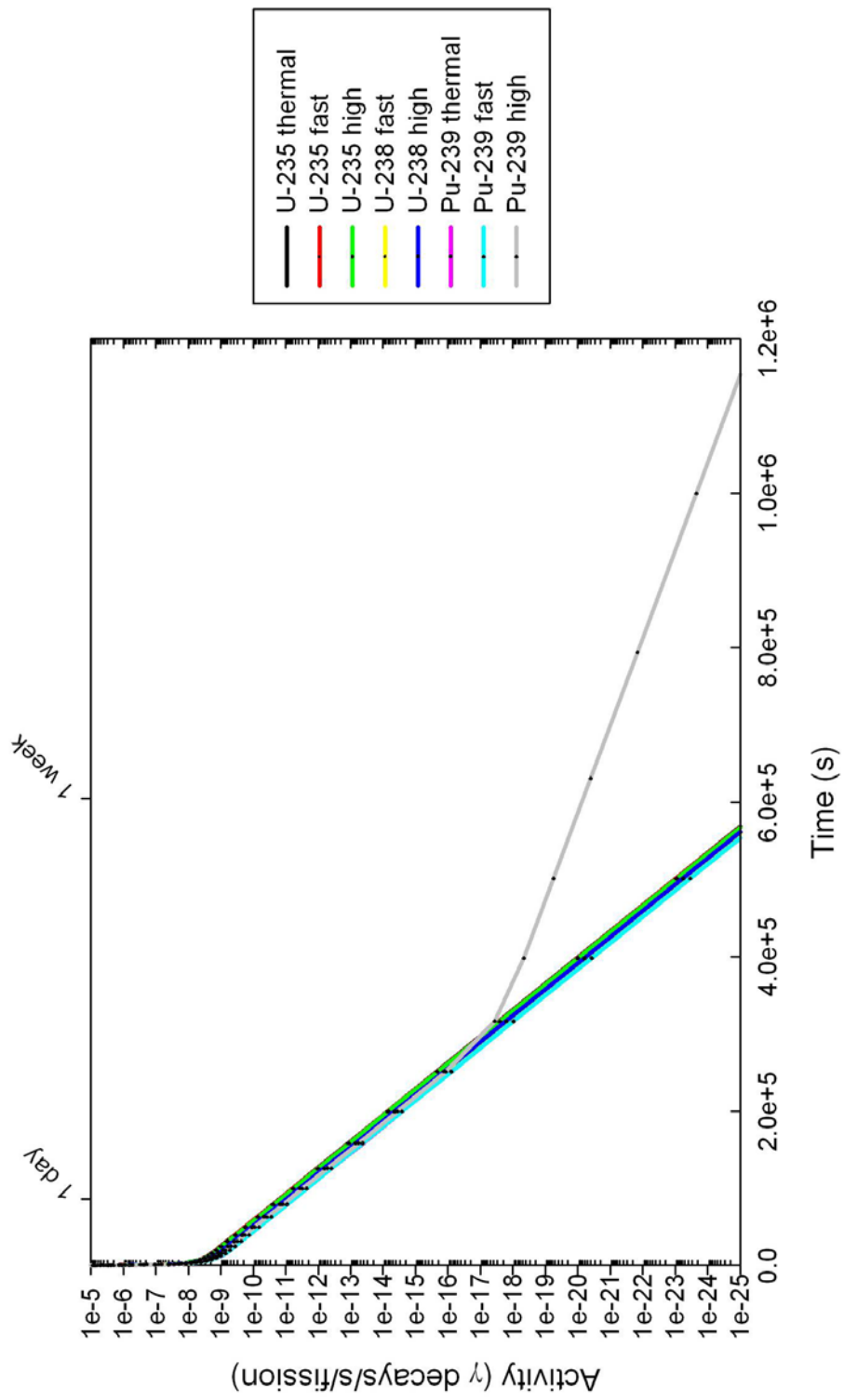


Figure 26 Gamma Activity, 4-5 MeV, 1 s to 1.2×10^6 s, Semi-Log

6. 5-6 MeV

The activities produced from fission in the 5-6 MeV range differ significantly from previously discussed energy bins. The different test cases are separated by the fuel type rather than incident neutron energy but U-235 now exhibits a greater activity than U-238. Pu-239 activity is still the lowest of any fuel. Figure 27 also shows an increase the activity for the U-238 fuels between 1.0 second and 10.0 seconds. Figure 28 shows this time scale in semi-log format to highlight the differences in the curves. The top five gamma intensity contributions to the activity at 1.0 second are all the result of the decay of Rb-92 ($t_{half} = 4.49$ s). The same analysis at 3.0 seconds yields the same result; the decay of Rb-92 is still responsible for the top five contributors to the total activity in the 5-6 MeV bin.

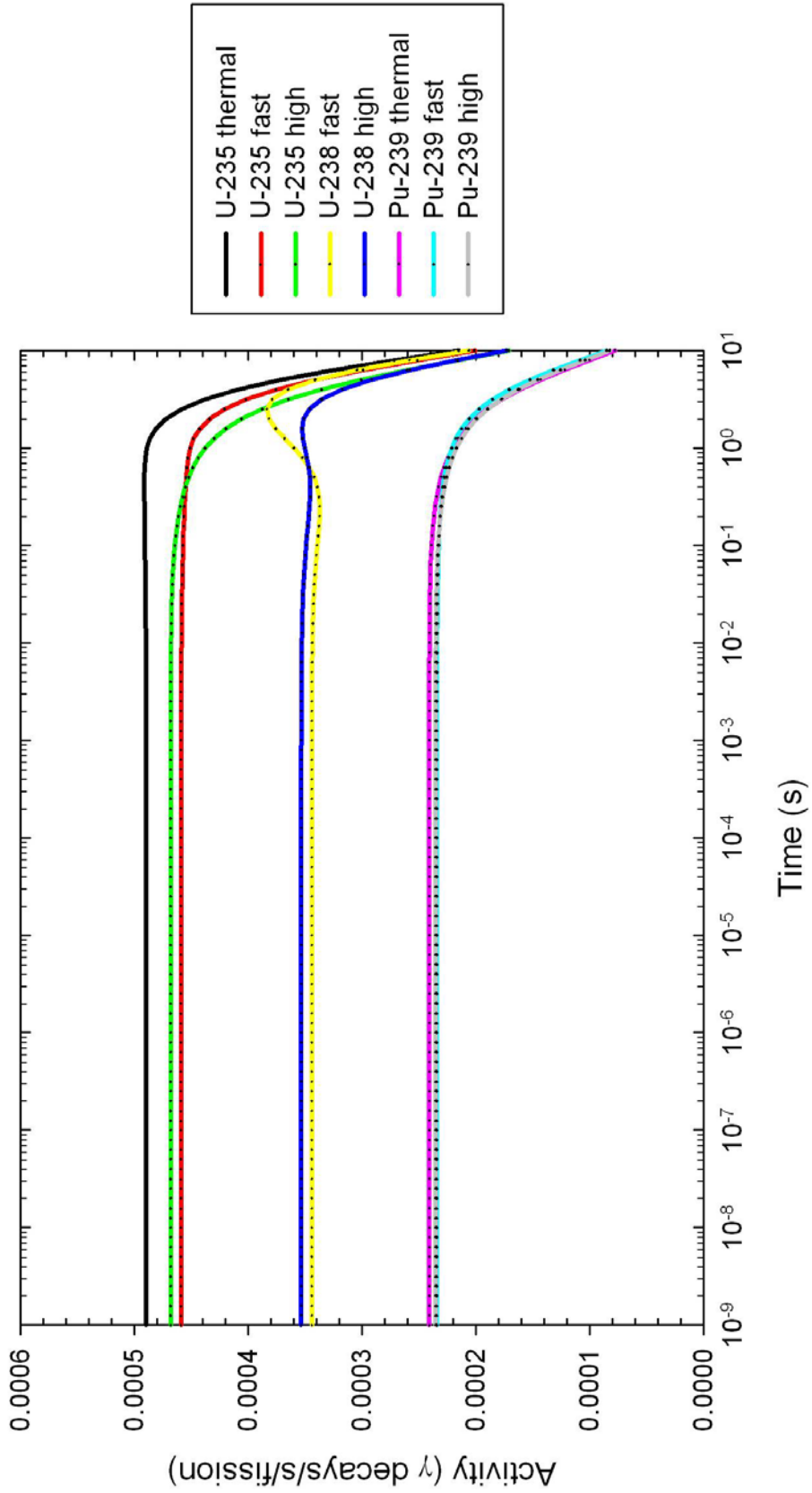


Figure 27 Gamma Activity, 5-6 MeV, 1 ns to 10 s, Log-Linear

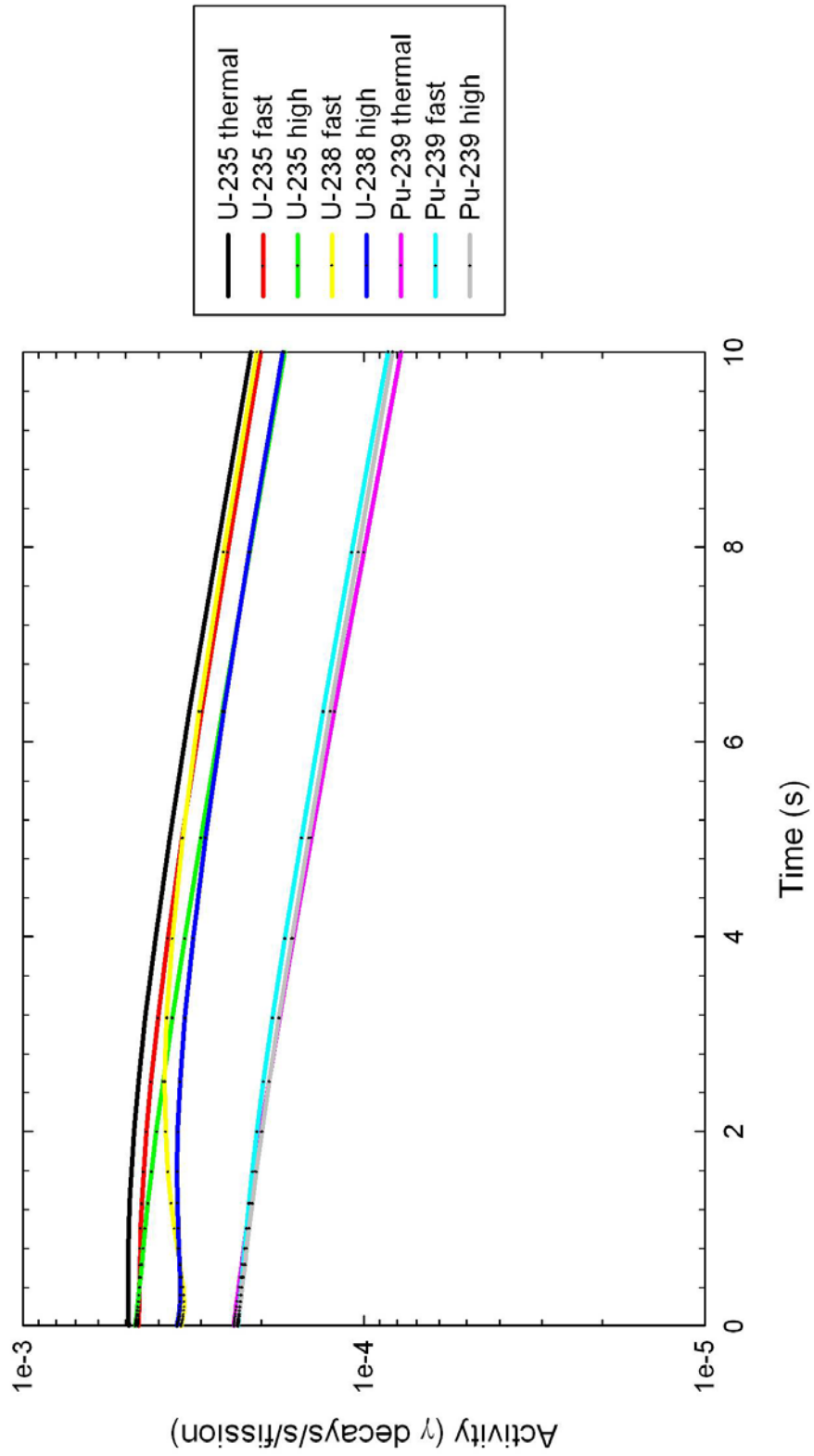
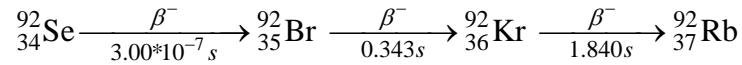


Figure 28 Gamma Activity, 5-6 MeV, 1 ns to 10 s, Semi-Log

The cause for the spike in activity in U-238 fast, and to a lesser extent U-238 high, is actually a result of the initial distribution of fission products. While relatively little Rb-92 is present initially in U-238 compared to U-235, the precursors to this isotope (only the direct decay branches are shown)



are present in greater quantities in U-238. The initial quantities as shown in Table 5 and the results after 3.0 seconds are shown in Table 6.

Table 5 Fission Product Yield per Fission Type

Isotope	Neutron Energy	Se-92 (t=0)	Br-92 (t=0)	Kr-92 (t=0)
U-235	thermal	4.17E-07	2.68E-04	1.66E-02
	fast	5.51E-07	2.09E-04	1.35E-02
	high	1.15E-06	3.03E-04	8.25E-03
U-238	fast	1.98E-05	2.34E-03	2.50E-02
	high	9.91E-06	1.34E-03	1.58E-02

Table 6 Rb-92 Quantity per Fission at t=0 s and t=3 s

Isotope	Neutron Energy	Rb-92 (t=0)	Rb-92 (t=3)
U-235	thermal	3.13E-02	2.85E-02
	fast	2.79E-02	2.49E-02
	high	2.93E-02	2.29E-02
U-238	fast	1.47E-02	2.33E-02
	high	1.89E-02	2.07E-02

Figure 29 shows an even more defined separation of Pu-239 activity following fission by a high energy neutron than demonstrated in the 4-5 MeV bin. The explanation for the difference is the same as above, namely the presence of Ga-66. Here, the only difference is that the activity in the other test cases is caused by the decay of Rb-90 as opposed to Rb-88 in the 4-5 MeV case.

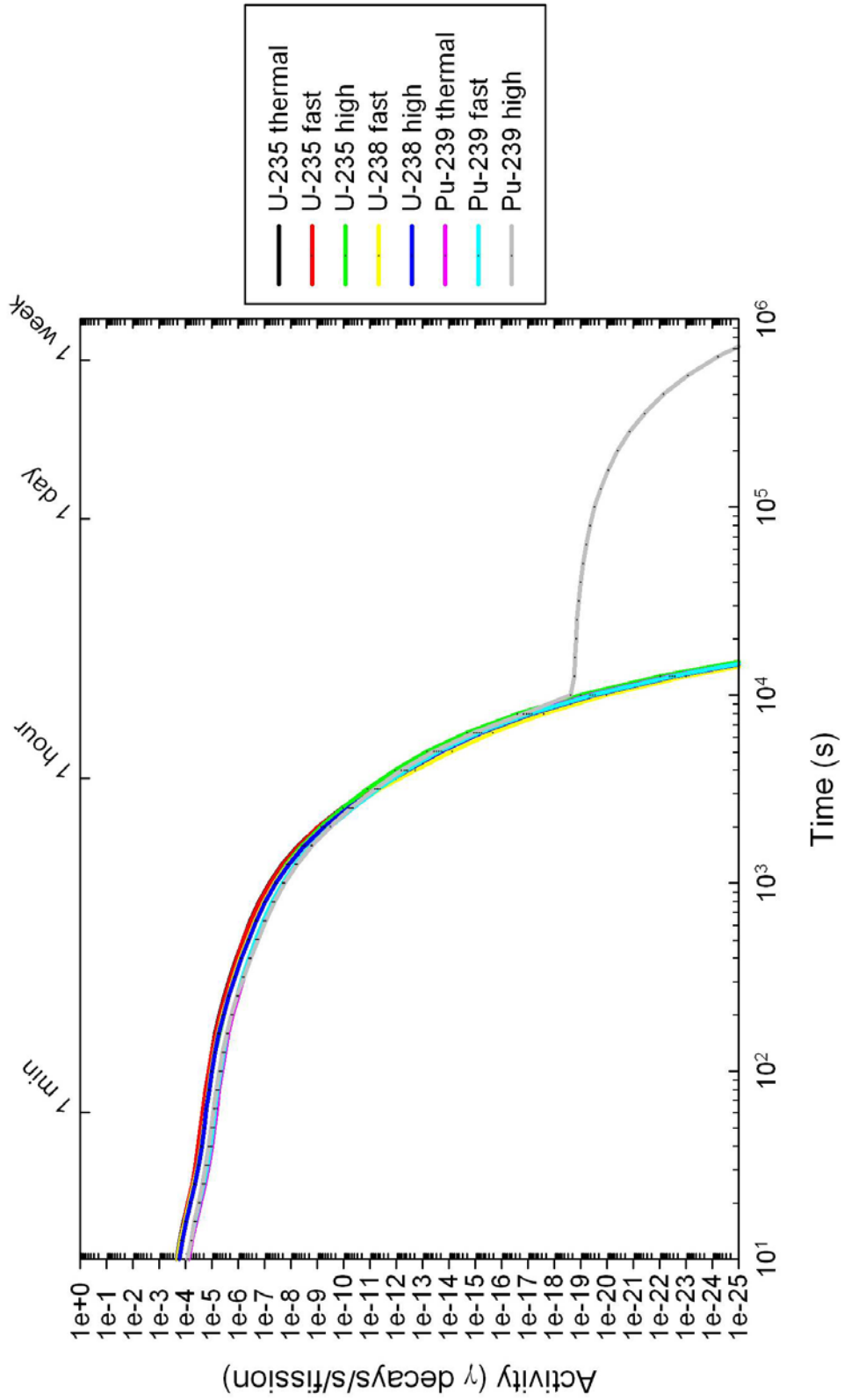


Figure 29 Gamma Activity, 5-6 MeV, 10 s to 10^6 s, Log-Log

7. 6-7 MeV

The 6-7 MeV energy bin activity displays many similarities to the 5-6 MeV bin. In fact, the activity at early times is due to the same isotope, Rb-92. The rest of the curve, as shown in Figure 31, depicts the activities from each of the different sources as largely indistinguishable. The semi-log plot in Figure 32 is more interesting because of the $t^{-1.2}$ plot as well as the closeness and straightness of the activity curves. The semi-log plot clearly shows that in the 6-7 MeV energy bin, the approximation is a poor fit for the data. The tight packing of the curves comes from all of the top five activity contributors being products of I-136 ($t_{half} = 83.4$ s) decay.

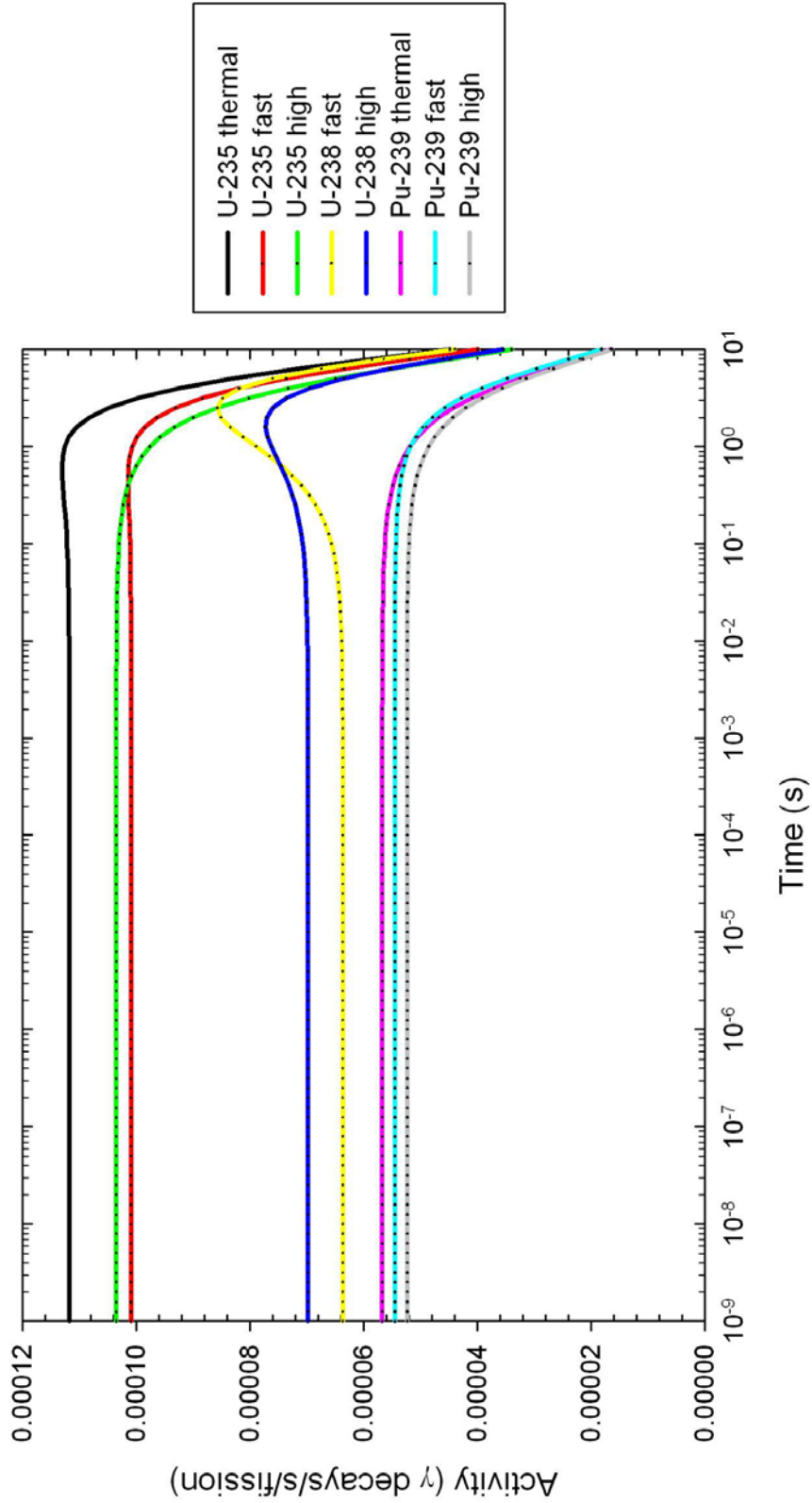


Figure 30 Gamma Activity, 6-7 MeV, 1 ns to 10 s, Log-Linear

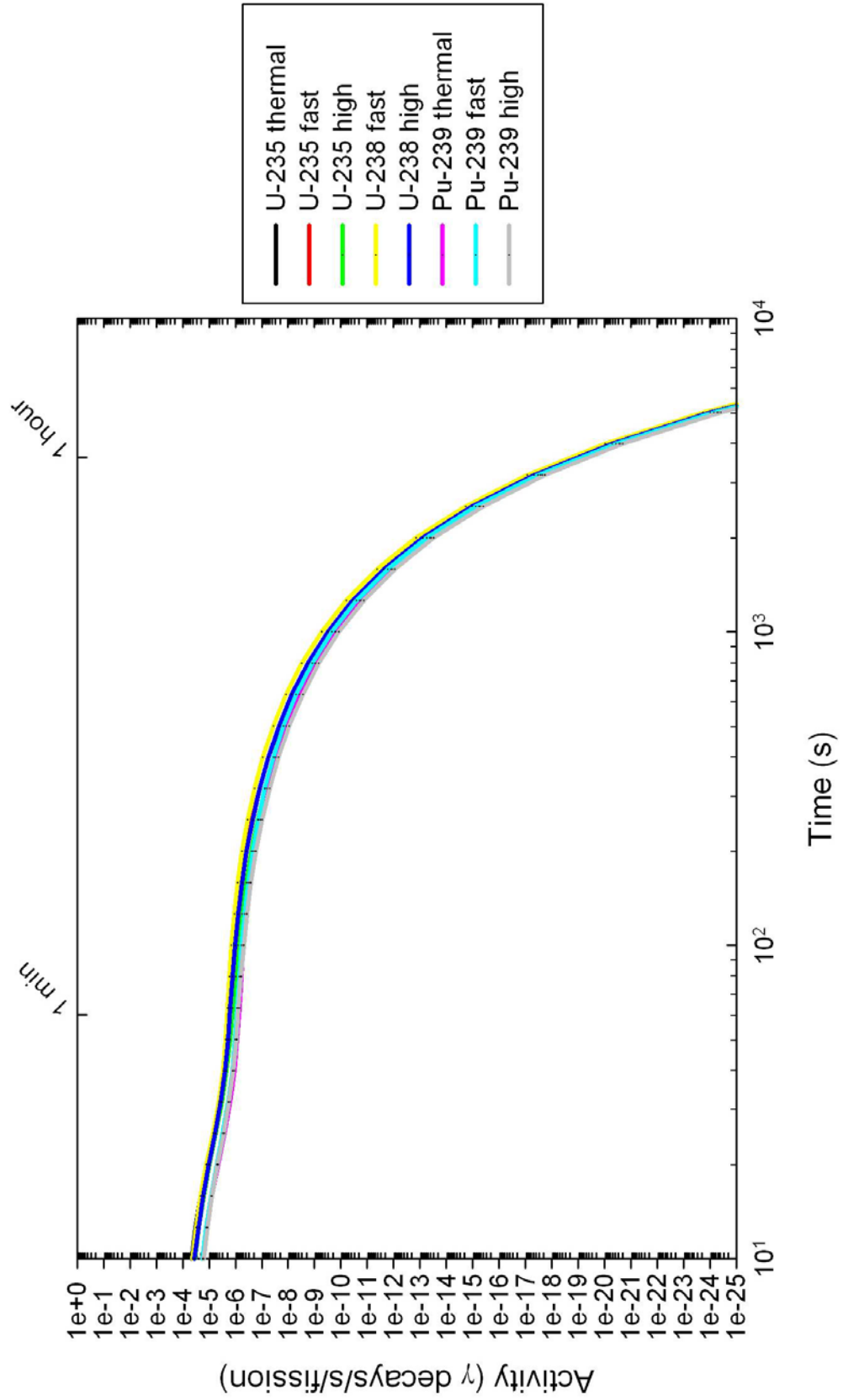


Figure 31 Gamma Activity, 6-7 MeV, 10 s to 10,000 s, Log-Log

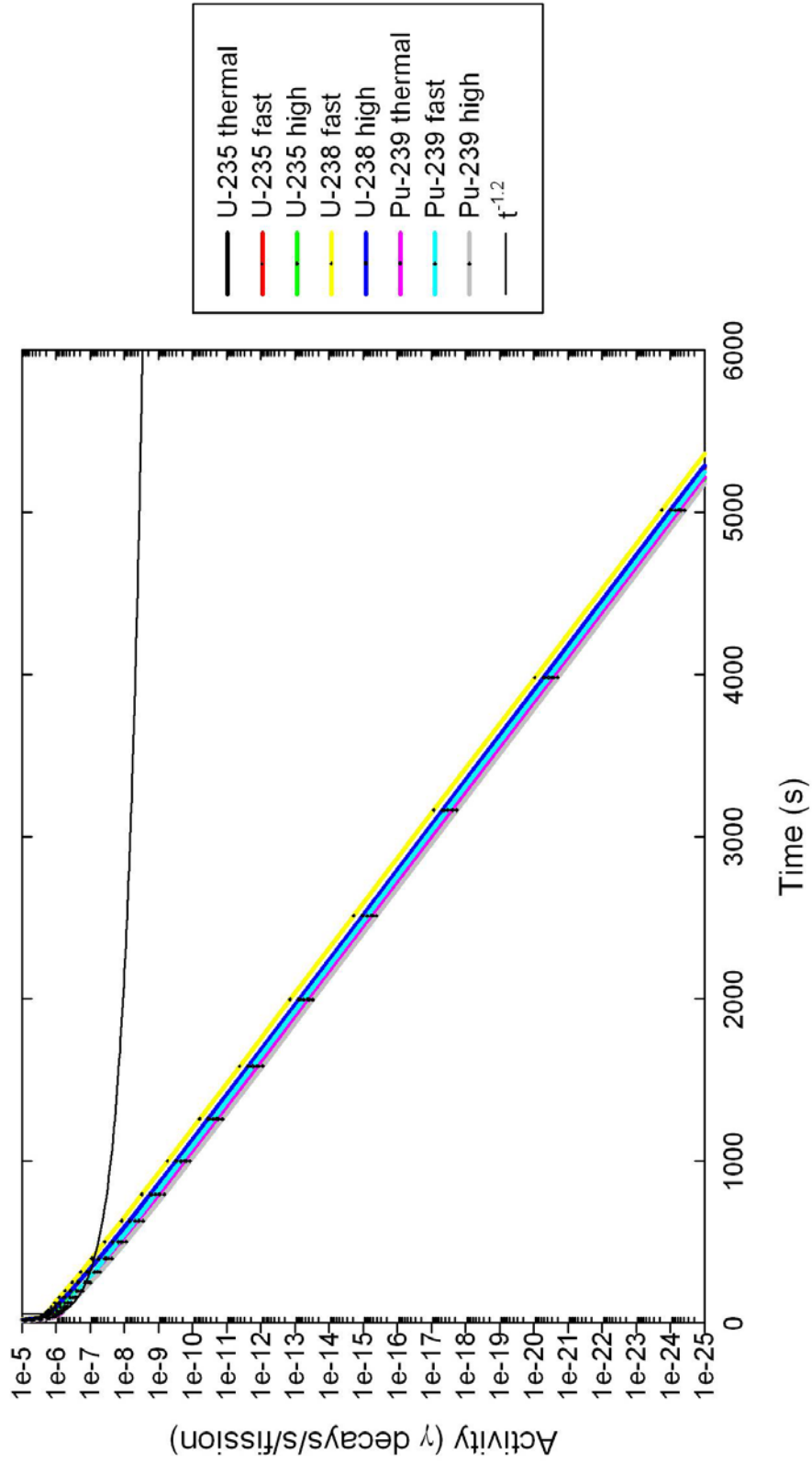
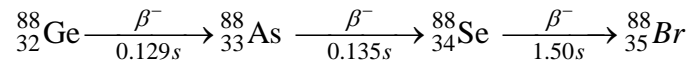


Figure 32 Gamma Activity, 6-7 MeV, 10 s to 6,000 s, Semi-Log

8. 7-8 MeV

The activity in the 7-8 MeV bin is unique in that for the test problems studied, the activity in this bin is the result of only one gamma ray from one isotope, the 7.000 MeV gamma emitted by the beta decay of Br-88 ($t_{half} = 16.29$ s).

The increase in activity after 1.0 second is due to the fission product yield. The fission product decays that result in the formation of Br-88 are shown below (only the direct decay chain is shown)



Se-89 ($t_{half} = 0.41$ s) also results in some production of Br-89 through a beta decay followed by a neutron emission. The combination of the A=88 chain with the Se-89 decay accounts for the increase in the activity of the U-235 and U-238 curves.

Figure 34 demonstrates again the application of the $t^{-1.2}$ approximation. The semi-log plot shows that the decay continues to be that of a single isotope, Br-88.

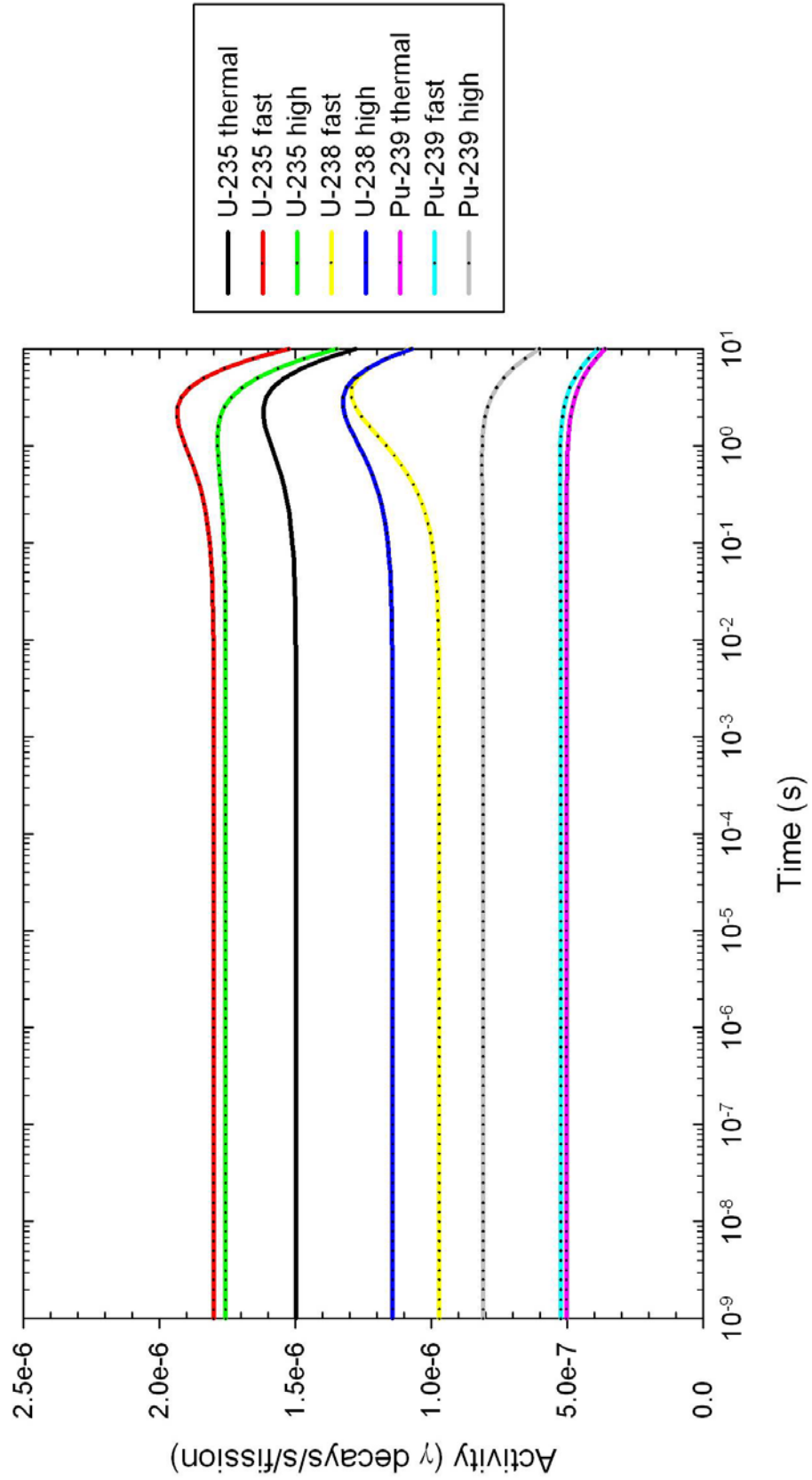


Figure 33 Gamma Activity, 7-8 MeV, 1 ns to 10 s, Log-Linear

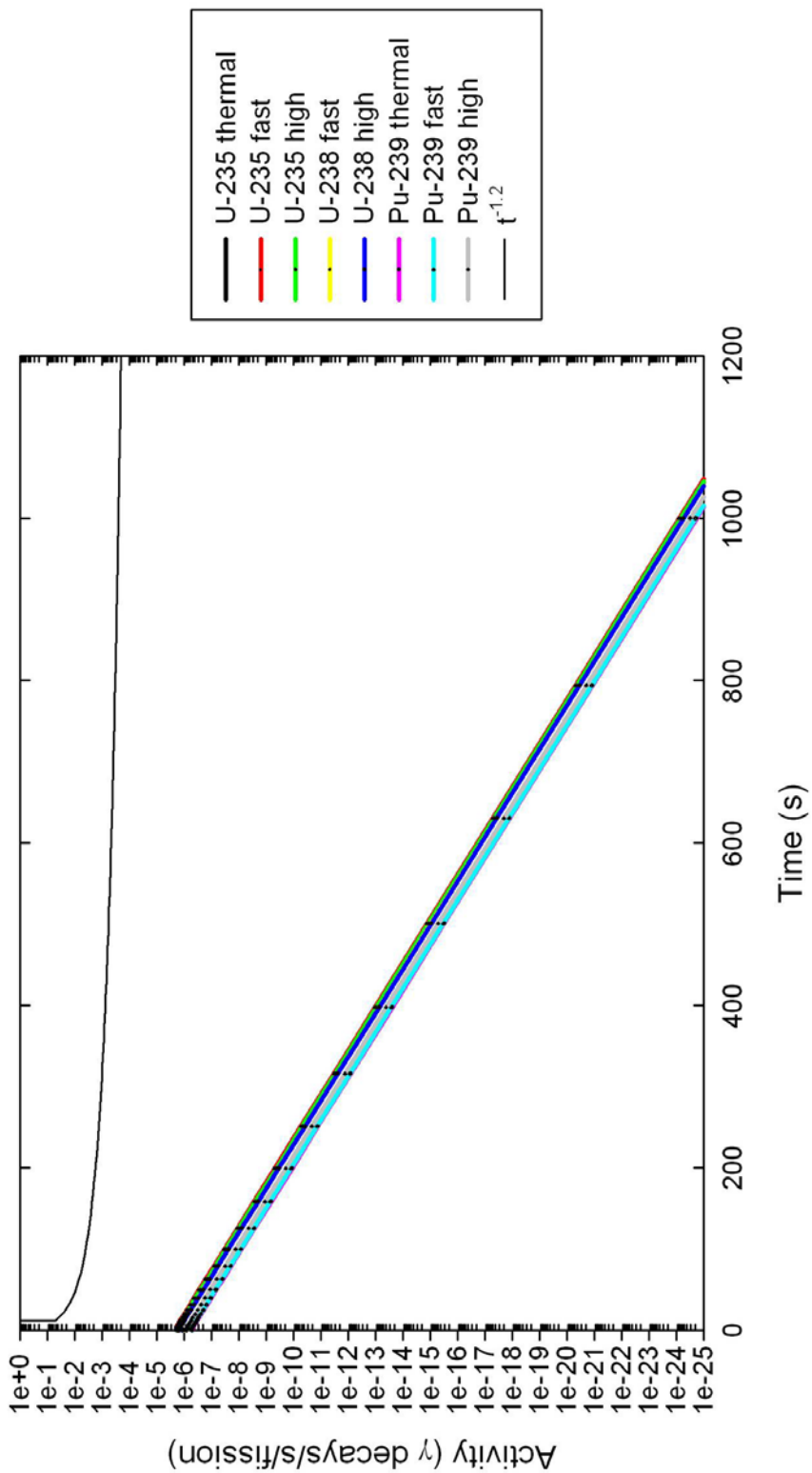


Figure 34 Gamma Activity, 7-8 MeV, 1 s to 1,200 s, Semi-Log

9. >8 MeV

Energy bins with minimum energies above 8.0 MeV do not have any activity for the test problems examined. Gamma radiation energies greater than this threshold are due to the decays of low Z materials (C-15, Na-20, Al-24, P-28, and K-36), which have a negligible probability of being a fission product.

VII. Conclusions and Recommendations

VII.A: Conclusions

The primary objective of this thesis was to produce a more precise code for calculating complex decay chains with greater precision than available by current methods. In implementing the exponential moments function with the use of a transmutation matrix, a code has been developed which gives the user access to quick and precise results for problems of as much complexity as desired. The code also provides insight into the effect on activity caused by the uncertainty of isotope data.

In implementing the exponential moments function, a proven mathematical model used in neutron transport calculations, the data was manipulated to provide the correct arguments necessary to calculate decay values. Verification of the method was performed by comparison to a Mathematica benchmark implementing the Bateman solution formula. The strong correlation between the two calculation methods gives strong indication that the exponential moments function is in fact accurate out to 10 digits when using double precision values in the calculation.

The use of a transmutation matrix is a novel way of approaching the decay chain problem. The matrices are stored in a sparse format which means that a library can be constructed to significantly reduce calculation time for some problem sets. The primary advantage of the T-matrix is that it allows the code to evaluate many different decay problems simultaneously.

This thesis also demonstrated one possible application of the exponential moments function combined with the use of a T-matrix. This approach proved a

worthwhile method that lead to an increased understanding of the activity emitted by fission products with respect to both energy and time.

The overall results of the thesis is that a method for calculating decay products with increased precision has been developed and can be adapted by the community where such a requirement is needed to better understand complex decay problems or where the uncertainty of gamma activity or isotope quantity is of interest.

VII.B: Recommendations for Future Work

To implement the exponential moments function calculations and generate T-matrices, certain assumptions had to be made to ensure that a working code could be made and thoroughly verified. Further exploration of some of these assumptions could produce even better results. Daughters of spontaneous fission decays were neglected in this code. Also, the treatments of metastable states in this thesis were not complete. Future work aimed at adding spontaneous fission decays and adding more realistic metastable state tracking and calculation should have the largest impact in improving performance even farther.

Further work in optimizing the exponential moments function to run faster would also be a benefit to the code. In addition, this code used the built in pseudo-random number generator that is part of Fortran 90/95. The implementation of a better pseudo-random number generator and performing more than 1000 runs would improve the results of the Monte Carlo simulation.

Appendix A: Order Invariance of Bateman Equation

The Bateman equation for the k^{th} isotope is given as

$$N_k(t) = N_1(0) \left(\prod_{i=1}^{k-1} b_{i,i+1} \lambda_i t \right) \sum_{j=1}^k \frac{e^{-\lambda_j t}}{\prod_{\substack{i=1 \\ i \neq j}}^k (\lambda_i t - \lambda_j t)} . \quad (\text{A.1})$$

I start the analysis by separating out two arbitrary isotopes from the decay chain, m and n.

$$N_k(t) = N_1(0) b_{m,m+1} b_{n,n+1} \lambda_m t \lambda_n t \left(\prod_{\substack{i=1 \\ i \neq m \\ i \neq n}}^{k-1} b_{i,i+1} \lambda_i t \right) * \quad (\text{A.2})$$

$$* \sum_{\substack{j=1 \\ j \neq m \\ j \neq n}}^k \frac{e^{-\lambda_j t}}{\prod_{\substack{i=1 \\ i \neq j}}^k (\lambda_i t - \lambda_j t)} + \frac{e^{-\lambda_m t}}{(\lambda_n - \lambda_m) \prod_{\substack{i=1 \\ i \neq m}}^k (\lambda_i t - \lambda_m t)} + \frac{e^{-\lambda_n t}}{(\lambda_m - \lambda_n) \prod_{\substack{i=1 \\ i \neq n}}^k (\lambda_i t - \lambda_n t)}$$

The next step is to swap m and n.

$$N_k(t) = N_1(0) b_{n,n+1} b_{m,m+1} \lambda_n t \lambda_m t \left(\prod_{\substack{i=1 \\ i \neq n \\ i \neq m}}^{k-1} b_{i,i+1} \lambda_i t \right) * \quad (\text{A.3})$$

$$* \sum_{\substack{j=1 \\ j \neq n \\ j \neq m}}^k \frac{e^{-\lambda_j t}}{\prod_{\substack{i=1 \\ i \neq j}}^k (\lambda_i t - \lambda_j t)} + \frac{e^{-\lambda_n t}}{(\lambda_m - \lambda_n) \prod_{\substack{i=1 \\ i \neq n}}^k (\lambda_i t - \lambda_n t)} + \frac{e^{-\lambda_m t}}{(\lambda_n - \lambda_m) \prod_{\substack{i=1 \\ i \neq m}}^k (\lambda_i t - \lambda_m t)}$$

Because equations (A.2) and (A.3) are equal, the Bateman equation is invariant with respect to order of the argument.

Appendix B: Depth-First Search Verification Test Problems

1. $A \rightarrow B$

2. $A \rightarrow B$
 $\rightarrow C$

3. $A \rightarrow B \rightarrow E$
 $\rightarrow C \rightarrow D \rightarrow E$

$A \rightarrow B$
4. $\rightarrow C$
 $\rightarrow D$

$A \rightarrow B \rightarrow D$
5. $\rightarrow B \rightarrow E$
 $\rightarrow C$

6. $A \rightarrow B \rightarrow D$
 $\rightarrow C \rightarrow D$

7. $A \rightarrow B \rightarrow D$
 $\rightarrow C \rightarrow E$

8. $A \rightarrow B \rightarrow C \rightarrow D \rightarrow E$

9. $A \rightarrow B \rightarrow C \rightarrow \dots \rightarrow T \rightarrow U$

Appendix C: Mathematica Verification Notebook

```

Off[General::spell1];
SetDirectory["C:\Thesis\Verify"];
problemData = Import["TestLambdas.csv", "CSV"];
i_max = Length[problemData]
strm = OpenWrite["answers.txt"];
starttime = AbsoluteTime[];
Do[
  λ[1] = N[10 $\frac{\text{problemData}[[i,1]]}{1001}$ , 300];
  λ[2] = N[10 $\frac{\text{problemData}[[i,2]]}{1002}$ , 300];
  λ[3] = N[10 $\frac{\text{problemData}[[i,3]]}{1003}$ , 300];
  λ[4] = N[10 $\text{problemData}[[i,4]]$ , 300];
  Do[
    bateman[k_] :=  $\left( \prod_{i=1}^{k-1} \lambda[i] \right) \left( \sum_{j=1}^k \frac{e^{-\lambda[j]}}{\left( \prod_{i=1}^{j-1} (\lambda[i] - \lambda[j]) \right) \left( \prod_{i=j+1}^k (\lambda[i] - \lambda[j]) \right)} \right);$ 
    b = bateman[k];
    Write[strm, FortranForm[N[b, 20]]];
    , {k, 4}
    , {i, i_max}
  stoptime = AbsoluteTime[];
  Close[strm];
  elapsedtime = stoptime - starttime
  Quit[];

```

Bibliography

1. Benedict, Manson, Pigford, Thomas, and Levi, Hans W., *Nuclear Chemical Engineering, Second Edition*, New York, McGraw-Hill, (1981).
2. Compaq Visual FORTRAN, Professional Edition 6.6.0. Verision 6.6.0, IBM, CD-ROM. Computer Software. Compaq Computer Corporation, (2000).
3. England, T. R. and Rider, B. F., "Evaluation and Compilation of Fission Product Yields," LA-UR-94-3106, ENDF-349, (October 1994).
4. England, T. R., Schenter, R. E., Whittemore, N. L., "Gamma and Beta Decay Power Following 235U and 239Pu Fission Bursts," LA-6021-MS, (July 1975).
5. Fission Home Page, Lawrence Berkeley National Laboratory, <http://www.ie.lbl.gov/fission.html>, (1998).
6. Herstein, I.N., Winter, David J., *Matrix Theory and Linear Algebra*, New York, Macmillan Publishing Company, (1988).
7. Mathews, Kirk A., personal communication, December 2006.
8. Mathews, Kirk A., Sjoden, Glenn, and Minor, Bryan, "Exponential Characteristic Spatial Quadrature for Discrete Ordinates Radiation Transport in Slab Geometry," *Nuclear Science and Engineering*, 118:24-37 (September 1994).
9. Mathematica, Version 5.2.0.0, Computer Software, Wolfram Research Inc., (2005).
10. Tuli, Jagdish K., Brookhaven National Laboratory, personal communication, October 2006.

REPORT DOCUMENTATION PAGE			<i>Form Approved OMB No. 074-0188</i>		
<p>The public reporting burden for this collection of information is estimated to average 1 hour per response, including the time for reviewing instructions, searching existing data sources, gathering and maintaining the data needed, and completing and reviewing the collection of information. Send comments regarding this burden estimate or any other aspect of the collection of information, including suggestions for reducing this burden to Department of Defense, Washington Headquarters Services, Directorate for Information Operations and Reports (0704-0188), 1215 Jefferson Davis Highway, Suite 1204, Arlington, VA 22202-4302. Respondents should be aware that notwithstanding any other provision of law, no person shall be subject to a penalty for failing to comply with a collection of information if it does not display a currently valid OMB control number.</p> <p>PLEASE DO NOT RETURN YOUR FORM TO THE ABOVE ADDRESS.</p>					
1. REPORT DATE (DD-MM-YYYY) 22-03-2007		2. REPORT TYPE Master's Thesis		3. DATES COVERED (From - To) Sep 2006 - Mar 2007	
4. TITLE AND SUBTITLE Precise Calculation of Complex Radioactive Decay Chains			5a. CONTRACT NUMBER		
			5b. GRANT NUMBER		
			5c. PROGRAM ELEMENT NUMBER		
6. AUTHOR(S) Logan J. Harr, Captain, USAF			5d. PROJECT NUMBER		
			5e. TASK NUMBER		
			5f. WORK UNIT NUMBER		
7. PERFORMING ORGANIZATION NAMES(S) AND ADDRESS(S) Air Force Institute of Technology Graduate School of Engineering and Management (AFIT/EN) 2950 Hobson Way WPAFB OH 45433-7765			8. PERFORMING ORGANIZATION REPORT NUMBER AFIT/GNE/ENP/07-03		
9. SPONSORING/MONITORING AGENCY NAME(S) AND ADDRESS(ES) Air Force Technical Applications Center Attn: Dr. Kirk Mathews AFIT/ENP 2950 Hobson Way Wright-Patterson AFB OH 45433-7765			10. SPONSOR/MONITOR'S ACRONYM(S) AFTAC		
			11. SPONSOR/MONITOR'S REPORT NUMBER(S)		
12. DISTRIBUTION/AVAILABILITY STATEMENT APPROVED FOR PUBLIC RELEASE; DISTRIBUTION UNLIMITED.					
13. SUPPLEMENTARY NOTES					
14. ABSTRACT This thesis documents a new approach to investigate the gamma radiation activity of the fission products of three different fuels (U-235, U-238, and U-239) exposed to three different incident neutron energy spectra (thermal, fast spectrum, and high energies). An application of the exponential moments function is used with a transmutation matrix in the calculation of complex radioactive decay chains to achieve greater precision than can be attained through current methods. The result of this research is a code which can calculate the decay products from complex radioactive decay chains with a high degree of precision while quantifying the uncertainty in gamma activity due to uncertainties in the isotope properties.					
15. SUBJECT TERMS Meeting Management, Delphi Technique, Malcolm Baldrige, Business Meetings, Management, Leadership Training, Organizational Meetings, Quality, Meeting Guide, Meeting Training, Management Training, Organizational Theory, Group Dynamics					
16. SECURITY CLASSIFICATION OF:		17. LIMITATION OF ABSTRACT	18. NUMBER OF PAGES	19a. NAME OF RESPONSIBLE PERSON	
REPORT	ABSTRACT			c. THIS PAGE	Kirk A. Mathews
U	U	UU	104	19b. TELEPHONE NUMBER (Include area code) (937) 255-3636, ext 4508; email: Kirk.Mathews@afit.edu	